Kinetic analysis of the interactions between Troponin C (TnC) and Troponin I (TnI) binding peptides: Evidence for separate binding sites for the 'structural' N-terminus and the 're...

ARTICLE *in* JOURNAL OF MOLECULAR RECOGNITION · JANUARY 2003

Impact Factor: 2.15 · DOI: 10.1002/jmr.606 · Source: PubMed

5 AUTHORS, INCLUDING:

Gregory De Crescenzo
Polytechnique Montréal
82 PUBLICATIONS **1,519** CITATIONS
SEE PROFILE

Robert S. Hodges
University of Colorado
497 PUBLICATIONS **21,519** CITATIONS
SEE PROFILE

JOURNAL OF MOLECULAR RECOGNITION
J. Mol. Recognit. 2003; **16**: 37–53
Published online in Wiley InterScience (www.interscience.wiley.com). **DOI**:10.1002/jmr.606

Kinetic analysis of the interactions between Troponin C (TnC) and Troponin I (TnI) binding peptides: evidence for separate binding sites for the 'structural' N-terminus and the 'regulatory' C-terminus of TnI on TnC

Brian Tripet[1], Gregory De Crescenzo[2], Suzanne Grothe[2], Maureen O'Connor-McCourt[2] and Robert S. Hodges[1]*

[1]Department of Biochemistry and Molecular Genetics, University of Colorado Health Sciences Center, Denver, Colorado, USA
[2]Biotechnology Research Institute, National Research Council of Canada, Montreal, Quebec, Canada

The Ca^{2+}/Mg^{2+}-dependent interactions between TnC and TnI play a critical role in regulating the 'on' and 'off' states of muscle contraction as well as maintaining the structural integrity of the troponin complex in the off state. In the present study, we have investigated the binding interactions between the N-terminus of TnI (residues 1–40 of skeletal TnI) and skeletal TnC in the presence of Ca^{2+} ions, Mg^{2+} ions and in the presence of the C-terminal regulatory region peptides: $TnI_{96–115}$, $TnI_{96–131}$ and $TnI_{96–139}$. Our results show the N-terminus of TnI can bind to TnC with high affinity in the presence of Ca^{2+} or Mg^{2+} ions with apparent equilibrium dissociation constants of $K_{d_{Ca2+}} = 48$ nM and $K_{d_{Mg2+}} = 29$ nM. The apparent association and dissociation rate constants for the interactions were, $k_{on} = 4.8 \times 10^5\ M^{-1}\ s^{-1}$, $3.4 \times 10^5\ M^{-1}\ s^{-1}$ and $k_{off} = 2.3 \times 10^{-2}\ s^{-1}$, $1.0 \times 10^{-2}\ s^{-1}$ for TnC(Ca^{2+}) and TnC(Mg^{2+}) states, respectively. Competition studies between each of the TnI regions and TnC showed that both TnI regions can bind simultaneously to TnC while native gel electrophoresis and SEC confirmed the formation of stable ternary complexes between $TnI_{96–139}$ (or $TnI_{96–131}$) and TnC–$TnI_{1–40}$. Further analysis of the binding interactions in the ternary complex showed the binding of the TnI regulatory region to TnC was critically dependent upon the presence of both TnC binding sites (i.e. $TnI_{96–115}$ and $TnI_{116–131}$) and the presence of Ca^{2+}. Furthermore, the presence of $TnI_{1–40}$ slightly weakened the affinity of the regulatory peptides for TnC. Taken together, these results support the model for TnI–TnC interaction where the N-terminus of TnI remains bound to the C-domain of TnC in the presence of high and low Ca^{2+} levels while the TnI regulatory region (residues 96–139) switches in its binding interactions between the actin-tropomyosin thin filament and its own sites on the N- and C-domain of TnC at high Ca^{2+} levels, thus regulating muscle contraction.

Keywords: **Troponin C; Troponin I; surface plasmon resonance; muscle regulation**

Received 27 August 2002; revised 25 October 2002; accepted 29 October 2002

INTRODUCTION

Vertebrate skeletal and cardiac muscle contraction is regulated by the concentration of Ca^{2+} via the regulatory protein complex, troponin (Tn), bound to the actin–tropomyosin thin filament. Troponin consists of the three proteins: troponin C (TnC), the Ca^{2+} binding subunit; troponin I (TnI), the inhibitory subunit; and troponin T (TnT), the tropomyosin (Tm) binding subunit. The binding of Ca^{2+} to TnC induces a conformational change which results in the release of the inhibitory effect of TnI and a change in the position of TnT–Tm on the actin thin filament to allow activation of the acto-myosin interaction and contraction (for recent reviews see Farah and Reinach, 1995; Houdusse *et al.*, 1997; Perry, 1999; Tobacman, 1996).

Understanding, at a molecular level, the protein–protein interactions and conformational changes which occur between members of the troponin complex in the presence and absence of Ca^{2+} has been a long-standing goal in muscle research. Although no published high-resolution structure of troponin has yet been forthcoming, a significant amount of progress has been made in elucidating the structure and/or functional properties of the individual subunits. For example, the structure of TnC has been solved by X-ray crystallography and NMR spectroscopy (Gagne *et*

*Correspondence to: R. S. Hodges, Department of Biochemistry and Molecular Genetics, University of Colorado Health Science Center, Biomedical Research Building, Rm 451, 4200 E 9th Ave, Denver, Co 80262, USA.
Contract/grant sponsor: Sensium Technologies Inc..
Contract/grant sponsor: University of Colorado Health Sciences Center, Denver.
Contract/grant sponsor: NIH ; *contract/grant number:* R01GM61855.

Abbreviations used: TFA, trifluoroacetic acid; Tn, troponin; TnC, troponin C; TnI, troponin I; TnT, troponin T; Tm, tropomyosin.

al., 1995; Herzberg and James, 1985; Houdusse *et al.*, 1997; Slupsky and Sykes, 1995; Strynadka *et al.*, 1997; Sundaralingam *et al.*, 1985). TnC is a highly α-helical protein which exists as a dumbbell-shaped molecule with two structurally independent globular domains linked by a long central helix (the D/E helix). Each domain possesses two metal-ion binding sites or EF hand motifs (Kretsinger and Nockolds, 1973). Binding studies have shown that the two metal binding sites within the N-terminal domain, sites I and II, bind Ca^{2+} ions specifically but with lower affinity than those of sites III and IV in the C-domain, which can bind Ca^{2+} and Mg^{2+} ions competitively (Potter and Gergely, 1975). In the initial X-ray structure of TnC, TnC showed Ca^{2+} ions bound only within the C-domain and thus revealed a relatively open conformation in the C-domain with an exposed hydrophobic patch and a closed conformation in the unoccupied homologous N-domain. In contrast, in the X-ray structure of the 4 Ca^{2+} TnC state (Houdusse *et al.*, 1997), the N-domain of TnC is observed to undergo a conformational change which re-orients the N, B and C helices (relative to the A and D helices) such that the N-domain now more closely mimics the C-domain, i.e. adopting an open conformation and exposing a new hydrophobic patch previously not exposed in the structure of TnC in the 2 Ca^{2+} state. Thus, it is presently believed that the structure of the 2 Ca^{2+} and 4 Ca^{2+} states may represent the 'relaxed' and 'activated' states of TnC in the troponin complex. Furthermore, based upon these and other studies, which have indicated the C-domain of TnC is likely to be continually occupied with metal ions under physiological conditions, the individual domains of TnC (N and C) are thought to play a 'regulatory' and 'structural' role, respectively. At present, no high-resolution structures exist for native TnI or TnT due to their apparent flexibility in the absence of complex formation.

In regards to functional analysis, studies have clearly established that the TnC–TnI interactions play a critical role in the Ca^{2+}-dependent regulatory process. TnI inhibits the Mg^{2+}-dependent actomyosin ATPase activity by binding to actin-Tm filaments, and the inhibitory interaction of TnI can be neutralized by the formation of a 1:1 complex with TnC in the presence of Ca^{2+} (Chong *et al.*, 1983; Syska *et al.*, 1976; Van Eyk and Hodges, 1988; Weeks and Perry, 1978). The inhibitory activity of TnI has been principally localized to a small 21-residue region located in the C-terminus of TnI (residues 96–116), termed the 'inhibitory region' (Syska *et al.*, 1976). Subsequent studies have shown that a synthetic peptide encompassing TnI residues 104–115 (referred to as the smallest inhibitory peptide) can bind to actin-Tm and inhibit the acto-S1-Tm ATPase activity as well as bind to TnC in a Ca^{2+}-dependent manner (Talbot and Hodges, 1981; Van Eyk and Hodges, 1988). Further, Van Eyk *et al.* (1993) have shown that this peptide can replace intact TnI in regulating the Ca^{2+}-dependent contraction and relaxation of skinned muscle fibers. Thus, it has been concluded that the Ca^{2+}-dependent switch between muscle contraction and relaxation involves a concomitant change of TnC from the 2 Ca^{2+} state to the 4Ca^{2+} state and a switch of the inhibitory region (residues 104–115) of TnI between actin-Tm and TnC (Van Eyk *et al.*, 1993).

In an effort to understand the interaction between TnC and TnI, considerable effort has been put into defining and characterizing the specific regions of the two proteins which make contact. Previous studies by Grabarek *et al.* (1981) using proteolytic fragments of TnC identified three regions of TnC (sites II, III and IV) which interact with TnI. Correspondingly, Syska *et al.* (1976) identified two regions of TnI which were capable of binding to a TnC-sepharose affinity column, the N-terminus (residues 1–47) and the C-terminus (residues 96–116) as discussed above. The N-terminus of TnI has been shown to bind exclusively to the C-domain of TnC in the presence of both Ca^{2+} or Mg^{2+} ions (Farah *et al.*, 1994; Luo *et al.*, 2000a; Ngai and Hodges, 2001a; Ngai and Hodges, 2001b). Also, very recently, a structure of whole TnC and TnI_{1-47} has been solved and shows that TnI residues 3–33 adopt an α-helical conformation which lies across the C-domain pocket covering the exposed hydrophobic patch (Vassylyev *et al.*, 1998). Functional studies have also shown that deletion of this region of TnI (TnIdel57) results in troponin complexes which are deficient in maintaining TnC in the low Ca^{2+}/Mg^{2+} state (Potter *et al.*, 1995; Sheng *et al.*, 1992). Based on these and other results it is thought that the N-terminus of TnI interacts with the C-domain of TnC to maintain TnC bound within the troponin complex.

Attempts to define the interaction interface between the C-terminal inhibitory region of TnI and TnC have been far less successful. Most evidence to date suggests that the inhibitory region interacts with residues 89–100 of TnC corresponding to the central helix and top of site III in the C-domain of TnC (Dalgarno *et al.*, 1982; Ding *et al.*, 1994; Drabikowski *et al.*, 1985; Grabarek *et al.*, 1981; Jha *et al.*, 1996; Kobayashi *et al.*, 1994, 1996, 1999a,1999b; Lan *et al.*, 1989; Leszyk *et al.*, 1987, 1988, 1998; Luo *et al.*, 2000b; Mercier *et al.*, 2000; Ngai *et al.*, 1994; Ramakrishnan and Hitchcock-DeGregori, 1995; Slupsky *et al.*, 1992; Swenson and Fredricksen, 1992; Tsuda *et al.*, 1992; Wang *et al.*, 1990; Weeks and Perry, 1978). Thus, these observations initially raised the interesting question as to how Ca^{2+} binding to the N-terminal regulatory domain (sites I and II) of TnC could regulate the binding interactions of the inhibitory region of TnI to the C-domain of TnC. More recent studies have, however, now shown that residues located adjacent to the C-terminus of the inhibitory region are also involved in the Ca^{2+}-dependent regulation of the inhibitory region (Farah *et al.*, 1994; Pearlstone *et al.*, 1997; Tripet *et al.*, 1997; Van Eyk *et al.*, 1997). For example, specific investigations by Tripet *et al.* (1997) using several synthetic peptides of the C-terminus of TnI have shown that residues 116–126, located adjacent to the 'inhibitory region' (residues 96–115), are critical for allowing TnC to neutralize fully and rapidly the acto-S1-Tm inhibition caused by the various TnI peptides. Furthermore, residues 116–131 of TnI (termed the 'TnC N-domain binding site' herein) can also significantly enhance the binding affinity of the inhibitory region, residues 96–115, for TnC in a Ca^{2+}-dependent manner as determined by affinity chromatography analysis and fluorescence spectroscopy (Pearlstone *et al.*, 1997; Tripet *et al.*, 1997). Thus, it is presently hypothesized that the Ca^{2+}-dependent switching of the inhibitory region between actin-Tm and TnC in intact TnI is regulated by the Ca^{2+}-dependent binding of residues 116–131 of TnI into and out of the N-terminal regulatory domain of TnC. Recent NMR

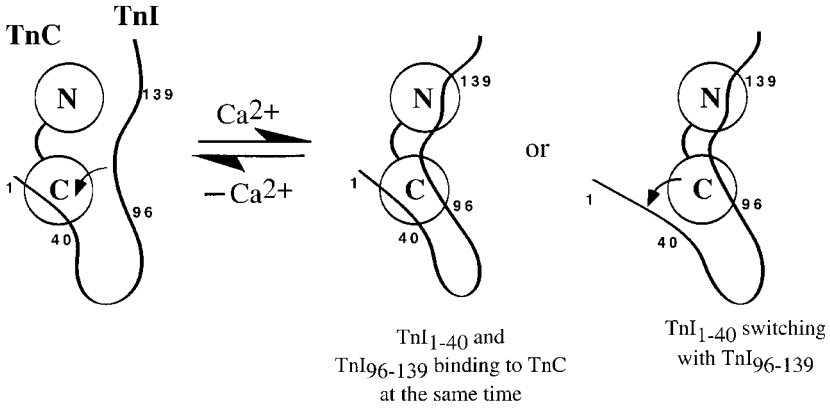

Figure 1. Schematic representation of the two hypotheses surrounding the binding interaction between the two different regions of TnI with TnC. TnC is depicted as a dumbbell shaped molecule with its globular N- and C-domains labeled N and C respectively. The central helix which interconnects the two domains is denoted by an inter-connecting black line. TnI is depicted as a long wavy black line with its various sequence regions denoted with numbers, e.g., 1, 40, 96 and 139. In the presence of Mg^{2+} ($-Ca^{2+}$), TnI residues 1–40 bind to the C-terminus of TnC. In the presence of Ca^{2+}, however, it is hypothesized that either (i) TnI residues 96–139 and 1–40 bind to the N- and C-domains of TnC at different sites of TnC (TnI_{1-40} and TnI_{96-139} binding to TnC at the same time) or (ii) TnI residues 96–139 bind to the N- and C-domains of TnC and displace residues 1–40, thus competing for the same binding site within the C-domain of TnC (TnI_{1-40} switching with TnI_{96-139}).

studies further support this model (Li *et al.*, 1999; McKay *et al.*, 1997, 1999).

One of the issues which has remained unclear in regards to the TnI-TnC organization is whether the C-terminal inhibitory region of TnI and the N-terminus of TnI have separate binding sites within the C-domain of TnC or whether they bind at the same site. Ngai and Hodges (1992) have shown that several synthetic peptides, TnI residues 1–40, 10–40 and 20–40 can block the ability of TnC to neutralize the inhibitory effects of the smallest inhibitory peptide or TnI in *in vitro* acto-myosin ATPase assays, demonstrating that the N-terminal region of TnI can negatively affect the ability of the inhibitory region to bind TnC and may be possibly competing for the same binding site within the C-domain of TnC. Mercier *et al.* (2000) have also studied the binding of the inhibitory region and the N-terminus of TnI with the C-domain of TnC (i.e. competition studies between $TnI_{96–115}$ and $TnI_{1–40}$ with the C-domain of TnC in the presence of Ca^{2+} as monitored by NMR spectroscopy) and observed $TnI_{1–40}$ and $TnI_{96–115}$ binding perturb similar residues in the C-domain and that $TnI_{96–115}$ can be out-competed by $TnI_{1–40}$ for binding to the C-domain. Similarly, Tripet *et al.* (1997) have also carried out competition studies between the N-terminus of TnI ($TnI_{1–40}$, residues 1–40) and the C-terminal peptides $TnI_{96–115}$, $TnI_{96–131}$, $TnI_{96–148}$ and TnI for binding to TnC and observed that $TnI_{1–40}$ could out-compete $TnI_{96–115}$ but not the other peptides. Based on their affinity chromatography and release assay results, Tripet *et al.* (1997) speculated that the binding between each TnI binding region (the N-terminus and C-terminus) could be significantly different in the presence of Ca^{2+} or Mg^{2+} conditions and thus the change in conditions could allow a mechanism by which the N-terminal region of TnI may be displaced by the greater affinity of the C-terminal regulatory domain in the presence of Ca^{2+}, due to its two-site-two-domain binding interaction; in contrast in the absence of Ca^{2+} (plus Mg^{2+}), the C-terminal regulatory domain of TnI is displaced off TnC by the N-terminus of TnI (Fig. 1, $TnI_{1–40}$ switching with $TnI_{96–139}$). In this model, $TnI_{1–40}$ could act as a facilitator for switching the inhibitory region back to the actin-Tm filament re-establishing inhibition.

In contrast, a variety of photochemical cross-linking and mutational studies have indicated the inhibitory region binding site and $TnI_{1–40}$ are different. For example, a TnC mutant in which sites III and IV have been knocked out (disrupting the C-domain) creates a TnC which is deficient in its ability to remain bound to troponin in the absence of Ca^{2+} yet can still carry out Ca^{2+} dependent regulation (Farah *et al.*, 1994; Sheng *et al.*, 1990; Sorenson *et al.*, 1995; Szczesna *et al.*, 1996). More recently, Luo *et al.* (2000a) have carried out photochemical cross-linking and distance measurements using FRET studies which show the N-terminus of TnI does not appear to move appreciably from the C-domain of TnC during Ca^{2+}-dependent release of the inhibitory region, hence arguing against a switching mechanism for $TnI_{1–40}$. Based on these and other results an alternate model has been proposed, one in which the N-terminus of TnI interacts with the C-domain of TnC in the presence of Ca^{2+} or Mg^{2+} and that release of the regulatory region ($\sim$ TnI residues 96–139) occurs independent of this interaction (Farah *et al.*, 1994) (Fig. 1, $TnI_{1–40}$ anchoring and $TnI_{96–139}$ switching).

One approach towards clearly establishing which of the two models is correct would be to determine accurately the equilibrium binding constants for each of the TnI binding regions alone and in combination with each other for TnC in the presence of Mg^{2+} and Ca^{2+} states. In this way, the change in affinity of each TnI binding region for TnC from a Mg^{2+} to Ca^{2+} state can be clearly understood as well as the

ability of one TnI region to out-compete the other in different metal ion states (one for TnI 1–40 and a different one for 96–131). Correspondingly, if binding involves two separate sites, are the binding sites independent from one another or does the binding involve cooperativity (positive or negative) where binding of one TnI region affects the binding ability of the other?

In a related manuscript (Tripet *et al.*, 2002) we determined the dissociation constants as well as the k_{on} and k_{off} rate constants for the TnI regulatory region peptides: $TnI_{96–131}$ and $TnI_{96–139}$ binding to TnC. In the present manuscript, we now extend these studies to include the binding interactions between $TnI_{1–40}$ and TnC. Using surface plasmon resonance (SPR)-based biosensor analysis, fluorescence spectroscopy, native gel electrophoresis and size-exclusion chromatography (SEC), we have determined the dissociation constants for the interaction between TnC and the N-terminus of TnI (residues 1–40) in the presence of Ca^{2+} ions, Mg^{2+} ions and in the presence of the C-terminal regulatory region peptides: $TnI_{96–115}$, $TnI_{96–131}$ and $TnI_{96–139}$. Our results show the N-terminus of TnI can bind to TnC with high affinity in the presence of Ca^{2+} or Mg^{2+} ions with apparent equilibrium dissociation constants of $K_{d_{Ca2+}} = 48$ nM and $K_{d_{Mg2+}} = 29$ nM, respectively. The apparent association and dissociation rate constants for the interactions were, $k_{on} = 4.8 \times 10^5$, 3.4×10^5 M^{-1} s^{-1} and $k_{off} = 2.3 \times 10^{-2}$, 1.0×10^{-2} s^{-1} for TnC (plus Ca^{2+}) and TnC (plus Mg^{2+}) states, respectively. Competition studies (between each of the TnI peptides and TnC) showed both of the TnI regions can bind simultaneously to TnC while native gel electrophoresis and SEC indicated the formation of stable ternary complexes between $TnI_{96–131}$ or $TnI_{96–139}$ and TnC and $TnI_{1–40}$. Further analysis of the binding interactions in the ternary complex showed that the binding of the regulatory region was critically dependent upon the presence of both TnC binding sites (i.e. $TnI_{96–115}$ and $TnI_{116–131}$) and the presence of Ca^{2+}, and that the presence of $TnI_{1–40}$ slightly weakened its affinity for TnC. Taken together, these results support the model for TnI–TnC interaction in the troponin complex where the N-terminus of TnI remains bound to the C-domain of TnC in the presence of high and low Ca^{2+} levels while the TnI regulatory region (residues 96–139) switches in its binding interactions between the actin–tropomyosin thin filament and its own sites on the N- and C-domain of TnC at high Ca^{2+} levels, thus regulating muscle contraction.

MATERIALS AND METHODS

Materials

Rabbit skeletal troponin C (TnC) was prepared according to the protocol detailed by Ingraham and Hodges (1988). Sensor chips (CM5, reagent grade), surfactant P20, 2-(2-pyridinyldithio) ethaneamine hydrochloride (PDEA), and the amine coupling kit containing N-hydroxysuccinimide (NHS) and 1-ethyl-3-(3-diethylaminopropyl)carbo-diimide (EDC) were obtained from Pharmacia Biosensor AB (Uppsala, Sweden). Cysteine hydrochloride was obtained from Bachem. All other chemicals were of analytical grade, and distilled water was used for all buffers.

Peptide synthesis

Peptides were prepared by solid-phase synthesis methodology using conventional *N-t*-butyloxycarbonyl (*t*-Boc) chemistry on an Applied Biosystems Model 430A peptide synthesizer. Peptides were cleaved from the resin by reaction with hydrogen fluoride (20 ml/g resin) containing 10% anisole and 2% 1,2-ethanedithiol for 1.5 h at 4°C. Crude peptides were washed with cold ether several times, and extracted from the resin with glacial acetic acid and lyophilized. Purification of each peptide was performed by reversed-phase HPLC (RP-HPLC) on a Zorbax semi-preparative C_8 column (250 × 10 mm i.d., 6.5 μm particle size, 300 Å pore size) with a linear AB gradient (ranging from 0.2 to 1.0% B/min) at a flow rate of 2 ml/min, where solvent A is aqueous 0.05% trifluoroacetic acid (TFA) and solvent B is 0.05% TFA in acetonitrile. Homogeneity of the purified peptides was verified by analytical RP-HPLC, amino acid analysis and electrospray quadrupole mass spectrometry.

$TnI_{1–40}$–E-coil conjugation

Covalent coupling of cysteine-containing $TnI_{1–40}$ peptides to the E-coil peptide was carried out by dissolving 1 mg of bromoacetylated-E-coil peptide (Br-E-coil, Table 1) in 400 μl of a 50 mM $KHPO_4$, 10 mM EDTA buffer, pH 7.2. TnI peptide (~1 mg/400 μl) dissolved in dH_2O (~pH 4) was then slowly titrated into the Br-E-coil solution until all of the Br-E-coil peptide reacted (as judged by RP-HPLC). The conjugate was then dialyzed extensively against several volumes of dH_2O and freeze dried.

K-coil immobilization

Covalent coupling of the cysteine containing K-coil peptide (Table 1) to the biosensor surface was carried using the ligand thiol method as described by Johnsson *et al.* (1991). Briefly, the dextran surface of the sensor chip was first activated with NHS/EDC (15 μl) followed by addition of PDEA (20 μl). K-coil (50 μg/ml) in 10 mM sodium acetate buffer pH 4.3 was injected and allowed to react to give a surface density of approximately 200–400 resonance units (RU, where 1 RU corresponds to an immobilized protein concentration of 1 pg/mm^2). Remaining activated groups were then blocked by injection (10 μl) of a 50 mM cysteine, 1 M NaCl, 0.1 M formate, pH 4.3 deactivation solution. All couplings were carried out using a running buffer which contained 10 mM HEPES pH 7.4, 100 mM NaCl, 3.5 mM EDTA and 0.05% P20.

Surface plasmon resonance analysis

All kinetic experiments were performed on a BIAcore™ 2000 instrument at 25°C. The instrument was programmed for iterative cycles in which each kinetic cycle consisted of (1) a 300 s TnC injection phase, (2) a 300 s dissociation phase, and (3) a 2 × 120 s regeneration phase. A flow rate of 5 μl/min was maintained throughout

Table 1. Amino acid sequences of the synthetic peptides used in this study

Peptide name	Substitution/modifications[a]	Sequence[b]
TnI_{1-40}		Ac-GDEEKRNRAITARRQHLKSVMLQIAATELEKEEGRREAEK-amide
$TnI_{1-40GGGC}$	GGGC	Ac-GDEEKRNRAITARRQHLKSVMLQIAATELEKEEGRREAEKGGGC-amide
TnI_{1-40ox}	M21M(O),GGGC	Ac-GDEEKRNRAITARRQHLKSV**M**LQIAATELEKEEGRREAEKGGGC-amide
K-coil		Ac-KVSALKEKVSALKEKVSALKEKVSALKEKVSALKEGG_nLC-amide
Br-E-coil		Br-Ac-EVSALEKEVSALEKEVSALEKEVSALEKEVSALEK-amide
TnI_{96-115}		Ac-NQKLFDLRGKFKRPPLRRVR-amide
$TnI_{115-131}$		Ac-RMSADAMLKALLGSKHK-amide
TnI_{96-131}		Ac-NQKLFDLRGKFKRPPLRRVRMSADAMLKALLGSKHK-amide
$TnI_{96-131ox}$	M(116,121)M(O)	Ac-NQKLFDLRGKFKRPPLRRVR**M**SADA**M**LKALLGSKHK-amide
$TnI_{96-131m}$	F106Y	Ac-NQKLFDLRGK**Y**KRPPLRRVRMSADAMLKALLGSKHK-amide
TnI_{96-139}	C133A	Ac-NQKLFDLRGKFKRPPLRRVRMSADAMLKALLGSKHKVAMDLRAN-amide
$TnI_{96-148Glysub}$	116-126G,C133A,T148G	Ac-NQKLFDLRGKFKRPPLRRVRGGGGGGGGGGGSKHKVAMDLRANLKQVKKEDG-amide

[a] Residues substituted or added to the native rabbit skeletal TnI. M(O) denotes methionine sulfoxide.
[b] Amino acid sequence of the peptides. Ac denotes N^{α}-acetyl and amide denotes C^{α}-amide. Methionine residues which exist as methionine sulfoxide are indicated in bold. Br denotes bromoacetyl. Residues added to the native sequence for site specific conjugation to the E-coil peptide are underlined. $_n$L denotes norleucine. m denotes the F106Y mutation.

Table 2. Summary of affinities and rate constants for TnC binding to immobilized TnI peptides

Peptide name[a]	Metal ion[b]	Binding[c]	k_{on} ($M^{-1}s^{-1}$)[d]	k_{off} (s^{-1})[d]	$K_{rearrangement}$[e]	K_d (M)[f]
TnI_{1-40}–EC	Ca^{2+}	(+)	4.8×10^5	2.3×10^{-2}	3.0	4.8×10^{-8}
TnI_{1-40}–EC	Mg^{2+}	(+)	3.4×10^5	1.0×10^{-2}	1.2	2.9×10^{-8}
$TnI_{1-40ox.}$–EC	Ca^{2+}	(NB)	—	—	—	—

[a] Name of TnI-E-coil peptide loaded to the biosensor surface.
[b] Metal ion (5 mM) present in running buffer.
[c] Ligand binding interaction with troponin C; (+) denotes sufficient binding interaction to calculate rate constants. NB = no and/or low binding which precluded accuracy of rate constant determination and calculation of affinity.
[d] k_{on} and k_{off} constants were obtained from nonlinear least squares global fitting of the respective sensorgrams using SP*Revolution* software version 2.0 and a model for conformational change.
[e] $K_{rearrangement} = k_2/k_{-2}$ (see Methods section).
[f] K_d (M) is the equilibrium dissociation constant derived from the rate constants k_{off} and k_{on} by the equation $K_d = k_{off}/k_{on}$.

the experiments. HEPES buffer saline (HBS) containing 10 mM HEPES pH 7.4, 100 mM NaCl, and 0.05% P20 plus 5 mM Ca^{2+} or Mg^{2+} (see Table 2 and Figure 2 legend) was used as the running and TnC buffer. An injection of 2×10 µl of HBS plus 4.5 mM EDTA was used to regenerate the surface prior to the next TnC injection. Loading of each TnI peptide–E-coil conjugate (50 µg/ml in HBS) was done in manual mode until the desired RU surface density was obtained (typically 50–100 RU). The concentration of TnC analyzed ranged from 10 to 300 nM (see figure legend) as determined by amino acid analysis. The SPR signal was recorded in real time with sampling at every 0.5 s and plotted as RU vs time (sensorgram). Each sensorgram was corrected for bulk refractive index changes by subtracting the corresponding TnC injection cycle on a blank K-coil derivatized surface.

SPR data analysis

The apparent association and dissociation rate constants (k_{on} and k_{off}, respectively) for the interaction between TnC and immobilized TnI peptides were calculated by globally fitting the data using different kinetic models available in the SP*Revolution* software package described in De Crescenzo *et al.* (2000, 2001). Two models were used: (1) a simple bimolecular Langmuir interaction, i.e. $A + B \rightleftharpoons AB$; and (2) a more complex model describing a kinetically limiting rearrangement of the complex after the initial binding, i.e.,

$$A + B \underset{k_{-1}}{\overset{k_1}{\rightleftharpoons}} AB \underset{k_{-2}}{\overset{k_2}{\rightleftharpoons}} AB^*$$

where AB is the first complex formed upon association of A

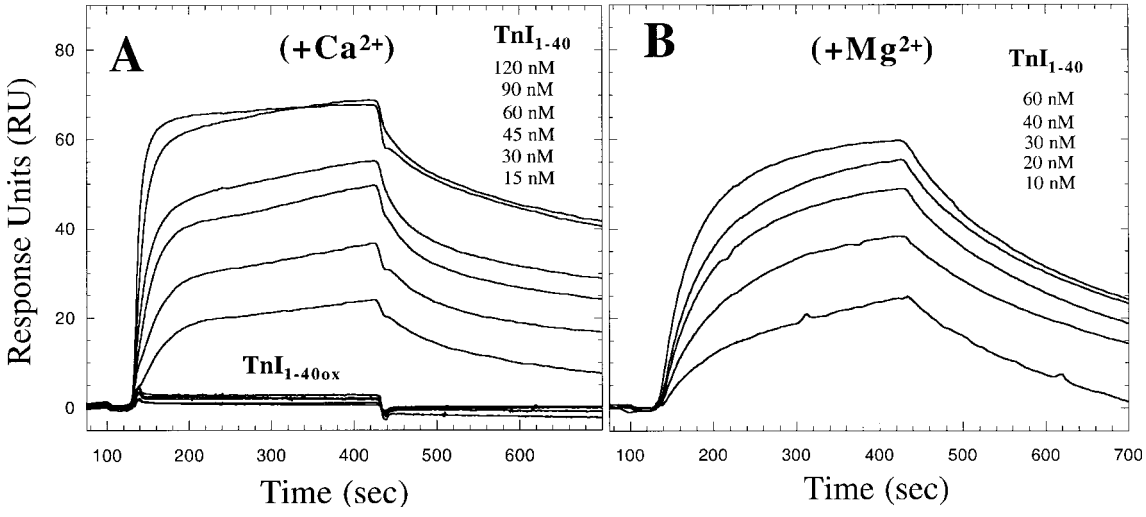

Figure 2. Kinetic analysis of TnC binding to TnI_{1-40} peptides at various TnC concentrations. The binding curves (sensorgrams) are expressed as resonance units (RU) as a function of time. TnC concentrations are given to the right of each trace in nM. Each analysis consisted of a 25 µl injection of TnC (association phase) in HBS plus 5 mM metal ion at a flow rate of 5 µl/min, 25 °C. Following injection, the dissociation phase was monitored with HBS plus 5 mM metal ion flowing over the sensor surface only. (A) TnC binding to TnI_{1-40}–EC and TnI_{1-40ox}–EC [containing methionine sulfoxide, denoted Met (O)] in the presence of 5 mM Ca^{2+} running buffer. Binding was observed only for the native reduced analog. (B) TnC binding to TnI_{1-40}–EC in the presence of 5 mM Mg^{2+} running buffer.

and B, which then undergoes a rearrangement to yield AB*. Thus, $k_{on} = k_1$, $k_{off} = k_{-1}k_{-2}/(k_2 + k_{-2})$, $k_{rearrangement} = k_2/k_{-2}$, and $K_d = k_{off}/k_{on}$. All the kinetic constants were global parameters (i.e. the same for all the curves) whereas the amount of captured $TnI_{1–40}$ was a local parameter (i.e. calculated independently for each curve).

IAEDANS labeling of TnC

Troponin C (TnC) from rabbit skeletal muscle was labeled with 1,5-IAEDANS (Molecular Probes) by incubating 4 mg (0.22 μmol) of TnC with 0.2 mg (0.44 μmol) of 5-({[(2-iodoacetyl)amino]ethyl}amino)naphthalene-1-sulfonic acid (1,5-IAEDANS) in 2 ml of 50 mM NH_4HCO_3, pH 7.5 buffer in the dark for 12 h. After quenching the reaction with excess dithiothreitol (DTT), the incubation mixture exhaustively dialyzed at 4 °C against 20 mM HEPES, 100 mM NaCl, pH 7.5 buffer containing either 5 mM $CaCl_2$ or 5 mM $MgCl_2$. A typical labeling ratio of 0.9 or greater label/TnC was observed.

Fluorescence studies

Fluorescence spectra were obtained with a Perkin-Elmer MFB-44B spectrofluorimeter equipped with a DCSU-2 corrected spectra accessory unit which allows automatic background fluorescence correction. The temperature of the cell was maintained at 25 °C using a Lauda RMS circulating water bath and an attached thermostated cell holder. The samples were measured in a semimicro 1 cm quartz cell, with a bandwidth of 5 nm used for both the excitation and emission monochrometers. The samples were excited at 340 nm, and the emission spectra recorded from 340–650 nm. For TnI peptide titrations in the presence of $TnI_{1–40}$, IAEDANS-labeled-TnC solutions (1 μM) were first pre-mixed with 8 μM of $TnI_{1–40}$, and then a 1–2 μl volume of TnI peptide stock solution (~125 μM) was added incrementally to the TnC–$TnI_{1–40}$ solution and the emission intensity spectra recorded. For $TnI_{1–40}$ peptide titration's in the presence of $TnI_{96–131}$, IAEDANS-labeled-TnC solutions (1 μM) were first pre-mixed with 1.6 μM of $TnI_{96–131}$, and then a 1–2 μl volume of TnI peptide stock solution (~125 μM) was added incrementally to the TnC–$TnI_{1–40}$ solutions and the emission intensity spectra recorded. Buffer conditions were 20 mM HEPES, 100 mM NaCl, pH 7.5 containing 5 mM $CaCl_2$ or 5 mM $MgCl_2$ (depending on the experiment).

Fluorescence data analysis

Calculation of the equilibrium dissociation constant for each TnI peptide–TnC titration by fluorescence spectroscopy was determined using the equation:

$$Y_i = (F_i - F_o)/(F_s - F_o)$$

where Y_i represents the fractional change in fluorescence for the *i*th addition of TnI peptide, F_i represents the observed fluorescence for the *i*th addition of TnI peptide, F_o represents the initial fluorescence in the absence of TnI peptide, and F_s represents the fluorescence at the TnI saturated state. The fractional change for each titration point (Y_i) was then plotted against the TnI peptide/TnC ratio, and the binding constant was determined by least-squares fitting of the data set to the equation:

$$Y_i = (X_i + P + K_d) - [(X_i + P + K_d)^2 - 4X_iP^{1/2}]/2P$$

where X_i and P represent the molar concentration of peptide (which was varied) and TnC (corrected for dilution) in the sample, respectively, and K_d is the TnI peptide dissociation constant to be determined. Note, curve fittings were carried out using both peak height and peak areas which gave similar results.

Non-denaturing gel electrophoresis

Analysis of the structural interactions of $TnI_{96–139}$ and $TnI_{1–40}$ with TnC was performed as detailed by Farah *et al.* (1994). Purified TnC (17.2 μM) was incubated at room temperature for 30 min with $TnI_{1–40}$ (17.2 and 68.8 μM), $TnI_{96–139}$ (17.2 and 68.8 μM) or a mixture containing each peptide (17.2 and 68.8 μM) in 20 mM HEPES, 100 mM NaCl, 5 mM $CaCl_2$, pH 7.5. Samples were then diluted with 1 vol of 41.5 mM Tris, 133 mM glycine (pH 8.6), 2 mM dithiothreitol, 0.02% bromophenol blue, 16% glycerol, and 10 mM $CaCl_2$. Samples were analyzed in an 8% native gel containing 25 mM Tris, 80 mM glycine (pH 8.6), 0.5 mM $CaCl_2$, and 10% glycerol.

Size-exclusion and reversed-phase chromatography

Mixtures of TnC (20 μg) and TnI peptides (e.g. $TnI_{1–40}$, $TnI_{96–139}$, or both; 0–20 μg) were dissolved in 100 μl of buffer consisting of 10 mM HEPES, 150 mM NaCl, 5 mM $CaCl_2$, 1 mM DTT at pH 7.5 and allowed to equilibrate at room temperature for 1 h. The TnC mixture was then loaded onto a high-performance size-exclusion column, Bio-Sil SEC-125 (7.8 mm i.d. × 30 cm; Bio-Rad Laboratories, Hercules, CA, USA) equilibrated in a buffer consisting of 10 mM HEPES, 150 mM NaCl, 5 mM $CaCl_2$, pH 7.5 at a flow rate of 0.7 ml/min and ambient temperature. The TnC peak was collected and analyzed by reversed-phase chromatography on an analytical C_8 column (Zorbax 300SB-C8, 15 cm × 4.6 mm i.d., 6.5 μm particle size, 300 Å pore size; Zorbax). The peptides and proteins were eluted from the column by employing a linear A-B gradient of 2% B/min, where eluent A is 0.05% aqueous TFA and eluent B is 0.05% TFA in acetonitrile (pH 2) at a flow rate of 1.0 ml/min at room temperature. To calculate the peptide/protein ratio in the complex, the peak areas of each constituent were compared with peak areas of known standard solutions of each peptide and TnC. For binding studies at higher salt conditions (i.e. 250 and 500 mM NaCl), TnC and peptide samples (as above) were dissolved in the same buffer with the exception that the salt concentration was increased.

RESULTS

Kinetics of TnC binding to the N-terminus of TnI (TnI residues 1–40)

To determine the kinetic rate constants (k_{on} and k_{off}) and equilibrium dissociation constants (K_d) for TnC binding to the N-terminus of TnI in the presence of Ca^{2+} or Mg^{2+} ions, experiments were conducted on an SPR-based biosensor (the BIAcore). In a typical SPR experiment, one of the binding partners was captured, in a covalent or non-covalent manner, on the sensor chip surface. The other binding partner was then injected in solution over the sensor chip surface. Specifically, a synthetic peptide corresponding to residues 1–40 of rabbit skeletal TnI (containing a Gly-Gly-Gly-Cys linker added at its C-terminus, see Table 1 for sequence) was conjugated to a Br-E-coil (EC) peptide as described in the Methods section. The $TnI_{1–40}$–EC conjugate was then captured on the biosensor surface through the E/K coiled-coil interaction until the amount of captured $TnI_{1–40}$–EC reached 50–150 RU. TnC (the analyte) was then injected over the immobilized $TnI_{1–40}$ surface at increasing concentrations and the interaction recorded. As observed in Fig. 2(A and B), TnC bound to the $TnI_{1–40}$ peptide in the presence of Ca^{2+} or Mg^{2+} ions in the running buffer but not in their absence (i.e. with running buffer containing 10 mM EDTA there was no change in the SPR signal; data not shown). The subtraction of the corresponding control sensorgrams (i.e. TnC injected over a similar surface where only E-coil peptide was captured) generated data sets which were then globally analyzed by curve-fitting with numerical integration methods using the SP*Revolution* software package (De Crescenzo *et al.*, 2000, 2001). Using this approach, the analysis of the sensorgrams gave a relatively poor fit when a simple 1:1 interaction model was applied (i.e. $> \pm 3$ RU for the fit residuals). However a better fit was observed using a conformational change model (i.e. $< \pm 2$ RU for the fit residuals) described by the equation: $A + B \rightleftharpoons AB \rightleftharpoons AB^*$. The calculated apparent k_{on} and k_{off} rate constants (Table 2) indicated the interaction of TnC (plus Ca^{2+}) with $TnI_{1–40}$ can be characterized as having a moderately fast on rate ($4.8 \times 10^5\ M^{-1}\ s^{-1}$) and a slow off rate ($2.3 \times 10^{-2}\ s^{-1}$) which generate a $K_d = 48$ nM. In the presence of Mg^{2+} ions, the kinetic rate constants and equilibrium dissociation constants K_d appear to be largely the same as those observed in the presence of Ca^{2+} ($k_{on} = 3.4 \times 10^5\ M^{-1}\ s^{-1}$; $k_{off} = 1.0 \times 10^{-2}\ s^{-1}$; $K_d = 29$ nM; Table 2). The largest difference observed between the two TnC binding states was in the rearrangement constant $K_{rearrangements}$ (~3-fold difference). The slightly faster rate to reach the bound state in the presence of Ca^{2+} may be reflecting the greater rigidity of the C-domain of TnC in the presence of Ca^{2+} versus the Mg^{2+} state.

To probe the specificity of the binding interaction between $TnI_{1–40}$ with TnC further, we analyzed the ability of TnC to bind the TnI analog $TnI_{1–40ox}$–EC. This analog contains methionine 21 oxidized to methionine sulfoxide (see Table 1 for sequence). Based on the recent X-ray structural analysis of $TnI_{1–47}$/TnC, Vassylyev *et al.* (1998) have shown that methionine 21 of TnI packs directly into the center of the hydrophobic pocket of the C-domain of

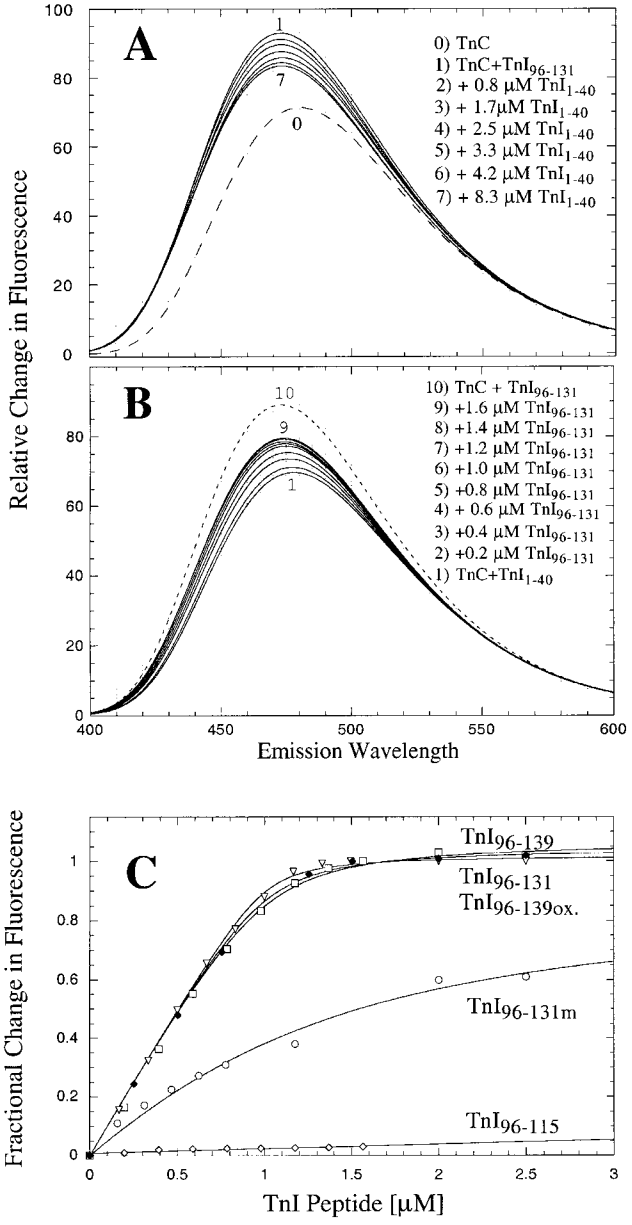

Figure 3. Competition studies between the N- and C-terminal regions of TnI for TnC. (A) Fluorescence emission spectra of Cys98 IAEDANS labeled TnC with increasing concentrations of $TnI_{1–40}$ in the presence of $TnI_{96–131}$. Excitation was at 340 nm. Buffer conditions were 20 mM HEPES, 100 mM NaCl, 5 mM $CaCl_2$, pH 7.5. TnC protein concentration was 1.1 μM, $TnI_{96–131}$ concentration (spectrum 1) was 1.6 μM, and the $TnI_{1–40}$ concentrations are indicated in the figure. The positions of the first and last spectra are indicated by the numbers 0 and 7, respectively. For example, spectrum 0 represents TnC apo; spectrum 1, TnC plus $TnI_{96–131}$; and spectra 2–7, TnC plus $TnI_{96–131}$ plus $TnI_{1–40}$. (B) Change in fluorescence emission spectra of Cys98 IAEDANS labeled TnC with increasing concentrations of $TnI_{96–131}$ in the presence of $TnI_{1–40}$. Excitation was at 340 nm. Buffer conditions were 20 mM HEPES, 100 mM NaCl, 5 mM $CaCl_2$, pH 7.5. TnC protein concentration was 1.1 μM, $TnI_{1–40}$ concentration 8 μM, and $TnI_{96–131}$ concentrations are indicated in the figure (spectra 2–9). The position of the first and last emission spectra in the titration are indicated by the numbers 1 and 9, respectively. Spectrum 10 (denoted by a dashed line) represents the emission spectrum of TnC–IAEDANS plus $TnI_{96–131}$ (1.6 μM) in the absence of $TnI_{1–40}$. (C) Binding curves derived from the change in fluorescence with TnI peptides; $TnI_{96–115}$, $TnI_{96–131}$, $TnI_{96–139}$, $TnI_{96–139OX.}$ and $TnI_{96–131m}$ binding to a preformed complex of TnC-$TnI_{1–40}$. The estimated dissociation constant for each binding curve is reported in Table 3.

Table 3. Summary of equilibrium dissociation constants derived from fluorescence spectroscopy for TnC–TnI peptide interactions

TnI peptide[a]	Receptor	Metal ion[b]	Binding[c]	K_d (M)[d]
$TnI_{1–40}$	$TnC/TnI_{96–131}$	Ca^{2+}	(+)	1.8×10^{-6}
$TnI_{96–115}$	$TnC/TnI_{1–40}$	Ca^{2+}	—	—
$TnI_{96–131}$	$TnC/TnI_{1–40}$	Ca^{2+}	(+)	1.1×10^{-7}
$TnI_{96–139}$	$TnC/TnI_{1–40}$	Ca^{2+}	(+)	6.5×10^{-8}
$TnI_{96–131ox.}$	$TnC/TnI_{1–40}$	Ca^{2+}	(+)	9.7×10^{-8}
$TnI_{96–115}$[e]	TnC	Ca^{2+}	(+)	3.8×10^{-7}
$TnI_{96–131}$[e]	TnC	Ca^{2+}	(+)	1.3×10^{-7}
$TnI_{96–139}$[e]	TnC	Ca^{2+}	(+)	5.6×10^{-8}
$TnI_{96–131ox.}$[e]	TnC	Ca^{2+}	(+)	8.7×10^{-8}
$TnI_{96–131m}$[e]	TnC	Ca^{2+}	(+)	1.4×10^{-7}
$TnI_{96–131m}$	$TnC/TnI_{1–40}$	Ca^{2+}	(+)	1.2×10^{-6}

[a] TnI peptide titrated to the solution of Cys98 IAEDANS labeled TnC or TnC–TnI peptide complex, column 2 (see Methods section for more details).
[b] Metal ion present in assay buffer (5 mM).
[c] Binding interactions with troponin C; (+) denotes binding interactions with TnC sufficient to allow calculation of an equilibrium dissociation constant; (—) denotes no, or insufficient binding interaction with TnC which precluded accurate determination of a K_d.
[d] Equilibrium dissociation constants (K_d) for TnC-TnI peptide interactions were determined by nonlinear least squares fitting of the change in fluorescence vs peptide concentration using the program Xcrvfit (available at www.pence.ualberta.ca).
[e] Affinities reported in Tripet *et al.* (2002) but shown here for direct comparison with the affinities of TnI peptides in the presence of $TnI_{1–40}$.

TnC, and thus its oxidation would be expected to disrupt and/or decrease significantly the tight packing interactions between the two molecules and hence result in a decrease in affinity which would easily be detected by the BIAcore analysis. BIAcore analysis for TnC binding to $TnI_{1–40ox.}$–EC in the presence of Ca^{2+} is shown in Figure 2 (A, bottom). In agreement with the $TnI_{1–47}$–TnC crystal structure complex (Vassylyev *et al.*, 1998), the binding between TnC and $TnI_{1–40ox}$ was significantly reduced such that its affinity was now lower than that which could be detected at the concentrations used in our BIAcore experiments (i.e. >μM).

Competition studies between the N- and C-terminal regions of TnI for TnC

To determine if both of the TnC binding regions of TnI (the N-terminus and the C-terminal regulatory region) can bind to TnC simultaneously or compete for the same site, we next analyzed the ability of TnC to bind to the $TnI_{1–40}$–EC surface in the presence of $TnI_{96–139}$ peptide in the running buffer during wash-on and wash-off phases. Attempts to acquire analyzable sensorgram data, however, failed due to the non-specific binding of the highly basic regulatory peptide to the carboxydextran matrix. In addition, TnC binding in the presence of $TnI_{1–40}$ peptide to a $TnI_{96–139}$–EC loaded surface also failed due to non-specific peptide binding to the dextran matrix.

In light of such results, we opted for a second approach. Having observed large changes in fluorescence for the binding of the TnI regulatory region peptides to IAEDANS-labeled TnC (Tripet *et al.*, 2002), we investigated whether addition of $TnI_{1–40}$ would displace the inhibitory region peptides (based on same site binding) and decrease the fluorescence which was induced by the latter's presence. To carry out these studies, we labeled TnC at position 98 with the cysteine specific IAEDANS fluoroprobe, added the appropriate amounts of TnI regulatory peptides to cause the maximal change in IAEDANS fluorescence, and then titrated $TnI_{1–40}$ to the complex and observed the change in fluorescence. A representative example of overlaid emission spectra is shown in [Figure 3(A)]. Addition of $TnI_{1–40}$ to $TnI_{96–131}$–TnC complex resulted in a decrease in the fluorescence quantum yield and a red shift in the spectra. This quenching and shifting is indicative that the fluoroprobe is now becoming more exposed and hydrated. Further additions of $TnI_{1–40}$ eventually resulted in only a 50% decrease of the enhancement of the probe (relative to the enhancement observed for addition of $TnI_{96–131}$ alone to TnC), after which further additions of $TnI_{1–40}$ did not affect the fluorescence, suggesting binding was complete and that a direct competition between the C-terminal region and the N-terminal region of TnI for a single site on TnC was not present. Similar results were also observed for the $TnI_{96–139}$, $TnI_{96–139ox}$ and $TnI_{96–131m}$–TnC complexes. Interestingly, however, the TnC–$TnI_{96–115}$ complex did show that it could be completely competed by the presence of $TnI_{1–40}$; that is, the entire fluorescence enhancement observed in the presence of $TnI_{96–115}$ alone was reduced to the point observed in its absence. This latter result would indicate that the $TnI_{1–40}$ region can modulate the binding interaction of $TnI_{96–115}$ for TnC such that in the absence of the C-terminal residues (TnI residue 116–131) its affinity is now below a necessary limit to continue to bind to TnC (at least under the assay conditions analyzed).

It should be noted that a larger than expected amount of $TnI_{1–40}$ peptide was required to achieve complete binding to the TnC–TnI regulatory peptide complexes than would have been expected based upon its high

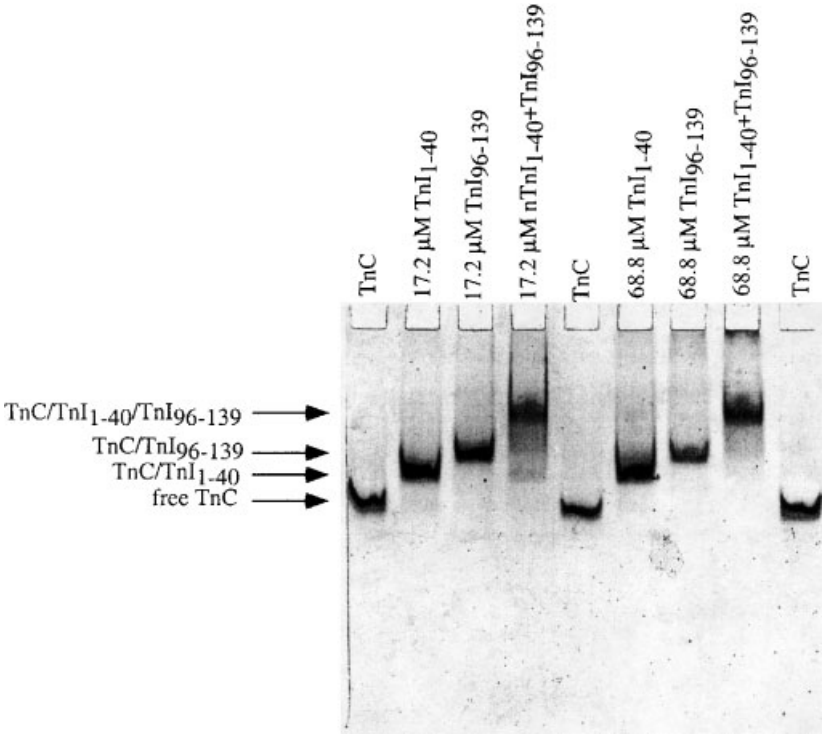

Figure 4. Analysis of interaction of $TnI_{1–40}$ and $TnI_{96–139}$ with purified TnC by polyacrylamide gel electrophoresis. Purified TnC (17.2 μM) was incubated at room temperature for 30 min with $TnI_{1–40}$ (17.2 and 68.8 μM), $TnI_{96–139}$ (17.2 and 68.8 μM), or a mixture of the two peptides $TnI_{1–40}$ + $TnI_{96–139}$ (17.2 and 68.8 μM), respectively. Samples were then diluted with 1 vol. of 41.5 mM Tris, 133 mM glycine (pH 8.6), 2 mM dithiothreitol, 0.02% bromophenol blue, 16.7% glycerol, and 10 mM $CaCl_2$. The samples were analyzed in an 8% native gel containing 25 mM Tris, 80 mM glycine (pH 8.6), 0.5 mM $CaCl_2$, and 10% glycerol and stained with Coomassie Brilliant Blue. Bands representing TnC and TnC complexes are indicated by the arrows.

affinity observed on the BIAcore. Calculation of the apparent binding affinity constant based upon the decrease in fluorescence vs concentration indicates a binding constant of 1.8×10^{-6} (Table 3), a 38-fold decrease compared with that observed on the BIAcore (Table 2). This significant decrease must arise from either steric interference by the probe on $TnI_{1–40}$ binding or binding of the TnI regulatory region ($TnI_{96–139}$) modulating the affinity of $TnI_{1–40}$.

As a second approach towards clarifying the presence or absence of a competition between $TnI_{1–40}$ and $TnI_{96–131}$ for TnC, TnC-IAEDANS was first pre-mixed with a high concentration of $TnI_{1–40}$ [i.e. the maximum concentration of $TnI_{1–40}$ which reduced the fluorescence in Fig. 3(A)] and then increasing concentrations of the C-terminal inhibitory region peptides were added. Interestingly, addition of $TnI_{1–40}$ to TnC-IAEDANS on its own resulted in no change in the emission spectra profile, and thus suggests that the binding of $TnI_{1–40}$ to TnC does not interact with, or change, the microenvironment of the IAEDANS probe attached at Cys 98 of TnC. In contrast, increasing additions of the TnI inhibitory region peptides (with the exception of $TnI_{96–115}$) resulted in an enhancement in the fluorescence emission spectra, e.g. an overlay of the emission spectra of $TnI_{96–131}$ at increasing concentration are shown in Fig. 3(B). The fluorescence enhancement increased with increasing concentration of inhibitory peptide up to a point equal in magnitude to one-half of the maximal fluorescence change possible in the absence of $TnI_{1–40}$ [compare spectra 9 and 10, Fig. 3(B)]. Further additions of TnI peptide resulted in no further increase in the emission spectrum. Plotting of the fractional change in fluorescence vs peptide concentration [Fig. 3(C)] and calculation of their binding constants showed that $TnI_{96–131}$, $TnI_{96–139}$ and $TnI_{96–131ox}$ can bind TnC with similar affinities to that observed in the absence of $TnI_{1–40}$ (Table 3). In contrast, the ability of $TnI_{96–131m}$ to bind TnC was now reduced by an order of magnitude (compare 1.4×10^{-7} with 1.2×10^{-6} M), and $TnI_{96–115}$ could not bind at all under the concentrations analyzed.

Taken together, the observation that the fluorescence change can only be modulated to a midway point in the presence of the two TnI regions, combined with the fact that each TnI region differs in their ability to affect the probe, supports a model for two different binding sites on TnC for the two TnI binding regions. Moreover, the fact that the binding affinity of $TnI_{96–115}$ and $TnI_{96–131m}$ peptides were modulated by the presence of $TnI_{1–40}$ also indicates there may be some allosteric or partial overlap near the inhibitory region's binding site.

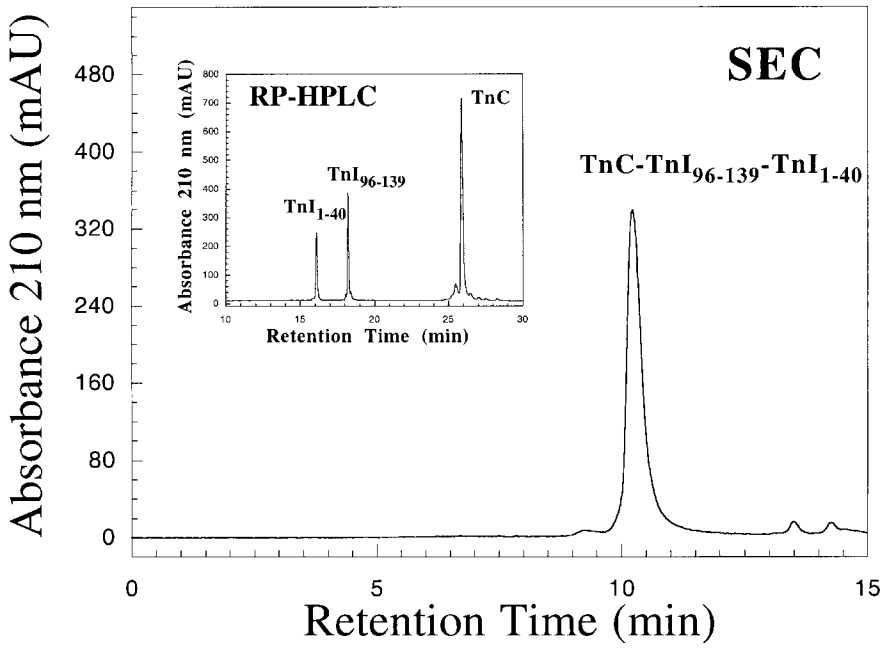

Figure 5. HPLC analysis of TnC-TnI peptides complex. TnC (1.2 nmol), $TnI_{1–40}$ (4.8 nmol) and $TnI_{96–139}$ (4.8 nmol) were pre-incubated together for 1 h in 100 μl running buffer and then applied to a BioRad Bio-Sil SEC-125 column equilibrated in a buffer consisting of 10 mM HEPES, 150 mM NaCl, 5 mM CaCl, pH 7.5, and a flow rate of 0.7 ml/min. The absorbance peak at 10.5 min corresponding to the TnC complex was collected and subsequently analyzed by reversed-phase chromatography (inset) on an analytical C_8 Zorbax column employing a linear A–B gradient of 2% B/min at 1 ml/min. Each RP-HPLC absorbance peak is labeled accordingly.

Analysis of the interaction between $TnI_{96–139}$, $TnI_{1–40}$ and TnC by polyacrylamide gel electrophoresis

To establish clearly whether both regions of TnI can associate with TnC simultaneously in a stable ternary complex, native gel polyacrylamide electrophoresis was carried out. In these studies, purified TnC was mixed with equal molar amounts of $TnI_{1–40}$ peptide, $TnI_{96–139}$ peptide, or an equal molar mixture of the two, and the products of the binding reactions resolved by non-denaturing gel electrophoresis (Fig. 4). In the presence of calcium, $TnI_{1–40}$ and $TnI_{96–139}$ both associate with TnC in a stable manner (lanes 2 and 3), as indicated by the presence of lower mobility (higher) bands and the absence of any free TnC. In the presence of both peptides at a 1:1:1 molar ratio to TnC, TnC now displayed a single band with even lower migration (lane 4), indicative of the formation of a stable complex which now contained both peptides simultaneously. To test further the stoichiometry of the interaction, similar complexes were prepared but at a 4:1 molar ratio of TnI peptides to TnC (Fig. 4, lanes 6–8). Lanes 6, 7 and 8 show bands that migrate similarly as those observed at the 1:1:1 complex ratios. Thus, the two TnI peptides bind TnC with a 1:1:1 stoichiometry.

Size-exclusion chromatography/RP-HPLC analysis $TnI_{1–40}$–$TnI_{96–139}$–TnC complexes

Based on the above results, which indicate TnC can interact in a stable manner with both TnI binding regions simultaneously, the interaction was studied further using size-exclusion chromatography (SEC) combined with RP-HPLC. TnC, $TnI_{1–40}$ and $TnI_{96–139}$ were incubated in the presence of Ca^{2+} at a 1:4:4 molar ratio and the mixture applied to a SEC column (Fig. 5). The complex was then collected and applied to a reversed-phased C_8 analytical HPLC column. The inset in Fig. 5, shows the RP-HPLC chromatogram. Both TnI peptides in addition to TnC were observed. Integration of the peak areas for each component and conversion of these values to mole amounts showed that the two peptides and TnC were present at a 1:1:1 mole ratio.

The ability of other peptides from the TnI regulatory region to form stable complexes with TnC and $TnI_{1–40}$ was also tested. No complex formation was observed for $TnI_{96–115}$, $TnI_{115–131}$ or $TnI_{96–148glysub}$, but was observed for $TnI_{96–131}$, indicating that both TnC binding sites within the regulatory region of TnI are necessary for the formation of a stable ternary complex with TnC–$TnI_{1–40}$ (data not shown). Moreover, none of the TnI regulatory region peptides were found to bind to the $TnI_{1–40}$–TnC complex when $CaCl_2$ was replaced by $MgCl_2$. Thus, the binding of the TnI regulatory region to TnC is clearly dependent upon the Ca^{2+} conformation of TnC (i.e. interaction with both domains). Note, $TnI_{1–40}$ was always observed to be bound to TnC in a 1:1 mole ratio in the presence of $MgCl_2$.

Distinctiveness of the binding sites of $TnI_{1–40}$ and $TnI_{96–139}$ on TnC

We next determined whether the binding of one TnI region to TnC could influence the affinity of the other. To carry out

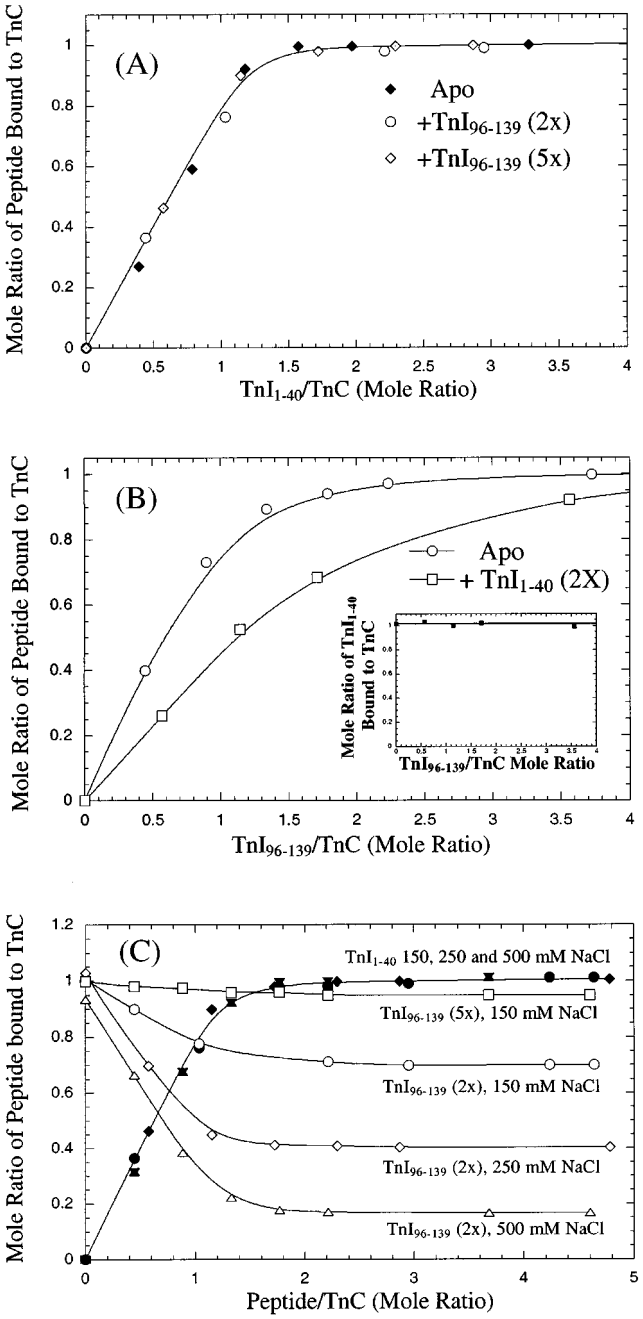

Figure 6. Study of the binding interactions between TnC and TnI peptides by SEC and RP-HPLC analysis. Complex formation and SEC and RP-HPLC runs were carried out as described in the Fig. 5 legend. (A) Molar ratio of observed $TnI_{1–40}$ peptide bound to TnC with increasing $TnI_{1–40}$ concentration in the absence (Apo) or presence [e.g. $+TnI_{96–139}(2\times)$ or $+TnI_{96–139}(5\times)$] of $TnI_{96–139}$. Note 2× and 5× refer to a 2:1 or 5:1 mole ratio of $TnI_{96–139}$:TnC in the starting complex mixture. (B) Mole ratio of observed $TnI_{96–139}$ peptide bound to TnC with increasing $TnI_{96–139}$ concentration in the absence (Apo) or presence of $TnI_{1–40}$ [+ $TnI_{1–40}$ (2×)]. Note 2× refers to a 2:1 mole ratio of $TnI_{1–40}$:TnC in the starting complex mixture. (B inset) The observed mole ratio of bound $TnI_{1–40}$ peptide to TnC in the presence of increasing $TnI_{96–139}$ peptide concentration (as shown in B). (C) Salt dependence of the TnI peptide–TnC complexes. Mole ratio of observed $TnI_{96–139}$ and $TnI_{1–40}$ peptides bound to TnC at different salt concentrations. Note 2× and 5× refer to a 2:1 or 5:1 mole ratio of $TnI_{96–139}$:TnC in the starting complex mixture. Buffer conditions were 20 mM HEPES (pH 7.5), 5 mM $CaCl_2$ and 150, 250 or 500 mM NaCl. All complexes were analyzed in the presence of calcium.

these studies, we chose to titrate individually one TnI peptide into a solution of either TnC alone or a pre-formed complex of TnC with the other TnI peptide. In the first series of experiments, increasing quantities of $TnI_{1–40}$ (0–4 nmol) were added to TnC alone or to a pre-incubated complex of TnC (1 nmol) and $TnI_{96–139}$ [2 nmol (2×) or 5 nmol (5×)], the mixture was then applied to a SEC column and the resulting TnC complex collected and resolved by analytical RP-HPLC (as above). The mole ratio of $TnI_{1–40}$ bound to TnC was then plotted vs its concentration relative to TnC. Figure 6(A) shows a binding curve indicative of a relatively high affinity interaction between the two molecules. For example, at a 1:1 mole ratio of $TnI_{1–40}$:TnC, 0.75 or 75% of the total $TnI_{1–40}$ was bound to TnC. At a 1.5 or greater mole ratio of $TnI_{1–40}$:TnC, a complete 1:1 complex was observed. Interestingly, the ability of $TnI_{1–40}$ to bind to TnC was independent of the presence of $TnI_{96–139}$. That is, the bound amount of $TnI_{1–40}$ to TnC in the presence of either a 2:1 or 5:1 mole ratio of $TnI_{96–139}$:TnC in the complex was superimposable.

The inverse experiment, i.e. analyzing the effect of $TnI_{1–40}$ pre-binding upon $TnI_{96–139}$–TnC complex formation [Fig. 6 (B)] was also done. $TnI_{96–139}$ binding to TnC alone showed that $TnI_{96–139}$ could form stable complexes with TnC with a similar affinity to that observed for $TnI_{1–40}$ [Fig. 6 (A)]. In the presence of a 2:1 molar ratio of $TnI_{1–40}$:TnC, the ability of $TnI_{96–139}$ to form a stable complex with TnC was significantly reduced [Fig. 6 (B)]. For example, at a 2:1 molar ratio of $TnI_{96–139}$:TnC, only 0.6 (60%) of the $TnI_{96–139}$ molecules were bound to TnC vs 0.95 (95%) in the absence of $TnI_{1–40}$. This difference is in contrast to the lack of effect of $TnI_{96–139}$ pre-binding upon $TnI_{1–40}$–TnC complex formation. Thus, this would suggest that the binding of $TnI_{1–40}$, although not affected by $TnI_{96–139}$, can negatively modulate the binding interactions between $TnI_{96–139}$ with TnC and hence weaken the affinity of $TnI_{96–139}$.

Salt dependence of the binding interaction between $TnI_{96–139}$ and TnC–$TnI_{1–40}$ complex

To investigate further the binding phenomena occurring during the formation of the ternary complex composed of $TnI_{1–40}$, $TnI_{96–139}$ and TnC, we analyzed the ability of $TnI_{1–40}$ to affect $TnI_{96–139}$ binding to TnC at different salt conditions [Fig. 6 (C), open symbols represent $TnI_{96–139}$ binding and solid symbols represent $TnI_{1–40}$ binding]. In the absence of $TnI_{1–40}$, $TnI_{96–139}$ showed an approximate 1:1 mole ratio of bound $TnI_{96–139}$ peptide to TnC, irrespective of salt concentration, indicating that in the absence of $TnI_{1–40}$ the interaction is insensitive to salt [Fig. 6 (C), *x*-axis = 0]. As $TnI_{1–40}$ is added, the amount of bound $TnI_{96–139}$ is reduced and this reduction is increased with salt concentration. For example, at a 2:1 mole ratio of $TnI_{1–40}$/TnC there is 0.75 (75%), 0.4 (40%), and 0.19 (19%) mole ratio $TnI_{96–139}$ bound to TnC at 150, 250 and 500 mM NaCl, respectively. At a higher $TnI_{96–139}$ peptide concentration [$TnI_{96–139}$ (5×)], this decrease can be reversed. It is interesting to note that the interaction between $TnI_{1–40}$ and TnC showed no dependence at all upon salt concentration.

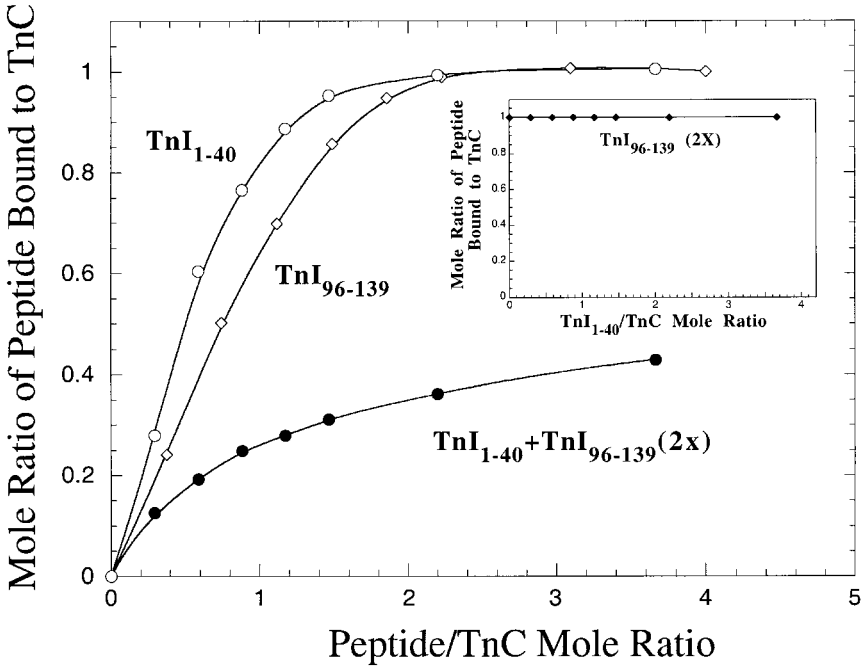

Figure 7. Binding of $TnI_{96–139}$ and $TnI_{1–40}$ to IAEDANS labeled TnC by SEC and RP-HPLC. TnC (1 nmol) labeled at position 98 with IAEDANS was mixed with $TnI_{96–139}$ (0–4.25 nmol), $TnI_{1–40}$ (0–4 nmol) or both in 100 μl buffer containing 10 mM HEPES, 150 mM NaCl, 5 mM Ca^{2+}, pH 7.5. The pre-incubated mixture (100 μl) was loaded onto the SEC column and the complex collected and loaded onto a Zorbax analytical reversed-phase column. Peak areas of each constituent of the complex were converted to mole amounts and their ratio relative to TnC is plotted. Note the curve labeled $TnI_{1–40}$ + $TnI_{96–139}$(2×) refers to TnC-IAEDANS complexes containing increasing concentrations of $TnI_{1–40}$ in the presence of a 2:1 mole ratio of $TnI_{96–139}$:TnC. Inset: The mole ratio of bound $TnI_{96–139}$ to TnC-IAEDANS in the presence of Ca^{2+} with increasing concentrations of $TnI_{1–40}$. See Materials and Methods section for conditions for the SEC and RP-HPLC runs.

Effect of the IAEDANS probe on the binding of $TnI_{1–40}$ to $TnI_{96–139}$–TnC

An observation made during the fluorescence analysis above was that the binding of $TnI_{1–40}$ peptide alone to TnC did not perturb the IAEDANS fluoroprobe at Cys 98; however, in the presence of the regulatory region peptides, $TnI_{1–40}$ could perturb the probe, but was also effectively reduced in its apparent affinity towards TnC. Since the affinity of $TnI_{1–40}$ is not reduced for TnC in the unmodified ternary complexes in the presence of $TnI_{96–139}$ as assessed by SEC and RP-HPLC above (ruling out a negative allosteric effect), we thus speculate that it is the forced positioning of the fluoroprobe after the inhibitory region binds (likely into the hydrophobic pocket) which results in steric blocking and/or disruption of the $TnI_{1–40}$ binding site. To verify if this is indeed the case, IAEDANS-labeled TnC was prepared and the ability of each of the TnI peptides to form a complex with TnC alone or together was analyzed by SEC and RP-HPLC as described above. As shown in Fig. 7, each of the individual peptides could still bind to IAEDANS-labeled TnC at similar ratios as that observed in the absence of the probe. In contrast, however, in the presence of a 2:1 mole ratio of $TnI_{96–139}$ peptide:TnC, the ability of $TnI_{1–40}$ to remain bound to the ternary complex was now significantly reduced (compare bound mole ratios of 0.35 vs 1 at a 2:1 peptide/TnC ratio, Fig. 7). Furthermore, increasing concentrations of $TnI_{1–40}$ peptide did not have any negative effect on the ability of the $TnI_{96–139}$ peptide to bind to IAEDANS-TnC (Fig. 7, inset), suggesting that the latter's affinity was now much greater than the $TnI_{1–40}$ peptide. Thus, these observations appear to be in agreement with the earlier fluorescence analysis (Fig. 3), which indicated an estimated 38-fold lower binding constant for $TnI_{1–40}$ in the presence of $TnI_{96–139}$ when TnC contains the fluoroprobe (Table 3). Moreover, the observation that no difference was observed in the binding curve of $TnI_{1–40}$ for TnC or IAEDANS-TnC in the absence of $TnI_{96–139}$ supports the idea that the probe is located away from the $TnI_{1–40}$ binding site in the absence of the inhibitory region but is then moved into its site, disrupting its binding, in its presence. Taken together, these observations show again that the binding interactions between the two regions of TnI for the C-domain of TnC are different.

DISCUSSION

The Ca^{2+}/Mg^{2+}-dependent interactions between TnC and TnI play a critical role in regulating the 'on' and 'off' states

of muscle contraction as well as maintaining the structural integrity of the troponin complex in the off state. In the present study, we have investigated the binding interactions between the N-terminus of TnI (residues 1–40 of skeletal TnI) and TnC in the presence of Ca^{2+} ions, Mg^{2+} ions, and in the presence or absence of the C-terminal regulatory region of TnI. We demonstrated that the N-terminus of TnI can bind with relatively high affinity to TnC in the presence of Ca^{2+} (48 nM) or Mg^{2+} (29 nM) but not in their absence. The observed minimal requirement for Mg^{2+} metal ions with TnC indicates that the $TnI_{1–40}$ peptide interaction is highly dependent upon the folded conformation of the C-domain of TnC (i.e. metal ions within the high-affinity metal ion binding sites III and IV of TnC). Thus, these results are in good agreement with previous studies which have reported similar observations (Farah *et al.*, 1994; Sorenson *et al.*, 1995). Moreover, the observation that $TnI_{1–40}$ can bind with similar affinities in both the presence of Ca^{2+} or Mg^{2+} ions suggests that the conformation of the C-domain of TnC is the same in the presence of either metal ion.

Interestingly, global fit analysis of the BIAcore data indicated a binding model which includes a conformational change after complex formation (vs a simple binding model). Although residues 1–40 are known primarily to bind the C-domain of TnC, the recent X-ray crystal structure of TnI1–47/TnC complex (Vassylyev *et al.*, 1998) indicates that there are some interactions between the N-domain of TnC and TnI1–47. Hence, the change in conformation that we observed may reflect this multiple contact site mode of binding between TnC and $TnI_{1–40}$.

Further investigations into the specificity of the $TnI_{1–40}$–TnC interaction has also revealed that the $TnI_{1–40}$ peptide is likely binding in these solution studies in a manner similar to that observed in the recent X-ray crystal structure of $TnI_{1–47}$/TnC complex (Vassylyev *et al.*, 1998), since oxidation of methionine 21 (to methionine sulfoxide), which is reported to play a critical role in the hydrophobic interactions between $TnI_{1–47}$ and TnC, did indeed display significant disruption in the binding interaction between $TnI_{1–40}$ and TnC, while modification of the cysteine residue 98 of TnC (by placement of the fluoroprobe IAEDANS) correspondingly resulted in an apparent weaker interaction in the presence of $TnI_{96–139}$ as assessed by fluorescence spectroscopy and size-exclusion chromatography.

Separate binding sites for $TnI_{1–40}$ and $TnI_{96–139}$ on TnC supports the structural domain hypothesis

Two models have been proposed to describe the interactions between the N- and C-terminal regions of TnI with the N- and C-terminal regions of TnC in the presence or absence of Ca^{2+} (see Fig. 1). The first one states that the N-terminus of TnI remains continuously bound to the C-domain of TnC while the C-terminal regulatory region of TnI (residues 96–139) dynamically switches between the thin filament and its own sites on the N- and C-domain of TnC depending on the concentration of Ca^{2+}. In contrast, the second model proposes that $TnI_{1–40}$ is bound to the C-domain of TnC in the absence of Ca^{2+} but then switches with the inhibitory region (TnI 96–115) in the presence of Ca^{2+} due to the Ca^{2+} dependent increase in affinity of the N-domain of TnC for TnI 116–131. In an attempt to clarify this issue further, we determined the ability of $TnI_{1–40}$ to displace competitively the regulatory region peptides from TnC in the presence of Ca^{2+} as assessed by fluorescence spectroscopy. As observed above, the results indicated that the addition of $TnI_{1–40}$ could only reduce the enhancement in the fluorescence emission spectrum caused by the binding of $TnI_{96–139}$ by 50%, suggesting a 1:1 binding of TnI peptides. Likewise, addition of the TnI regulatory peptides to pre-mixed TnC/$TnI_{1–40}$ complex resulted in 50% enhancement of the fluorescence of the probe (relative to TnC alone), and this binding best fit a 1:1 binding scheme with apparent affinities similar to those previously observed in the absence of the $TnI_{1–40}$ peptide. Hence, competition between the two TnI peptides for the same site within the C-domain of TnC does not appear to be the case. Moreover, the observation that modification of cysteine 98 of TnC (by the fluoroprobe) only reduced the affinity of $TnI_{1–40}$ and not that of the TnI regulatory region peptides in the complex, also supports a model for separate binding sites in the C-domain of TnC.

Additionally, we showed using non-denaturing gel electrophoresis and SEC-RP-HPLC analysis that both TnI regions ($TnI_{1–40}$ and $TnI_{96–139}$) can bind to TnC simultaneously in the presence of Ca^{2+}, resulting in a stable ternary complex with a 1:1:1 stoichiometry. Importantly, the latter technique also showed that the interaction between the C-terminal regulatory region of TnI with TnC was critically dependent upon Ca^{2+} and interaction with both domains of TnC. Thus, these results support the first $TnI_{1–40}$ anchoring model.

In light of these results, we can now understand better our previous competition assays. For example, Tripet *et al.* (1997) showed that $TnI_{1–40}$ was unable to displace significantly $TnI_{96–131}$, $TnI_{96–148}$ or TnI protein from TnC. This can now be explained by the fact that $TnI_{1–40}$ was binding simultaneously but at a different site. Further the marginal release that was observed can be ascribed to $TnI_{1–40}$'s negative binding effect (see below).

Further support for a separate binding site model can be drawn from the recent results of Tao's group which used fluorescence resonance energy transfer (FRET) and photochemical cross-linking between TnC and TnI and observed little change in the location of the N-terminus (residue 6) of TnI in the C-domain of TnC in either the presence of Ca^{2+} or Mg^{2+} ions (Luo *et al.*, 2000a). Thus, these results support the binary complex model between TnC and TnI in which the N-terminal region remains bound to the C-domain of TnC in the presence of high and low Ca^{2+} concentrations, while the C-terminal regulatory region of TnI dynamically switches on or off TnC (both domains) depending on the concentration of Ca^{2+}.

$TnI_{96–115}$ binding to TnC

It is interesting to note that, although the above results strongly support a model for separate binding sites between the N-terminal 'structural' and C-terminal 'regulatory' regions of TnI with TnC, the presence of TnI residues 1–

40 with TnC ($TnI_{1–40}$ added initially or after) completely eliminated the ability of the smaller TnI inhibitory region peptide ($TnI_{96–115}$) to bind to the C-domain of TnC in the presence of Ca^{2+}. One possible explanation for the $TnI_{96–115}$ observation, however, may be that the two binding sites on TnC are different yet not mutually exclusive. That is, the binding of one can influence the other. Consistent with this explanation is the observation that the binding of $TnI_{1–40}$ does cause a slight decrease in the binding ability of the longer regulatory region peptides ($TnI_{96–131}$ and $TnI_{96–139}$ as assessed by SEC-RPHPLC); thus, in the particular case of $TnI_{96–115}$, its affinity may have just been reduced to a point that is now below the detectable limit of the binding assay (i.e. it does not have enough interactions to remain bound in the presence of $TnI_{1–40}$). It is not the case that the inhibitory region site is blocked, because all of the longer TnI regulatory analogs, which contain more residues to their C-terminus, were able to interact with the C-domain of TnC. Moreover, even in the presence of Mg^{2+}, which is expected to eliminate the N-domain interaction of TnC with these analogs (making them more like $TnI_{96–115}$), all of the longer TnI regulatory analogs (e.g. $TnI_{96–131}$ and $TnI_{96–139}$) were still able bind to TnC in the presence of $TnI_{1–40}$ (as assessed by fluorescence, data not shown). Thus, it would appear that only a few additional interactions (particularly towards the C-terminus) are necessary in order to bring the binding ability of the inhibitory region peptide back above the minimal threshold of detection in order to observe this interaction.

Thus, one could ask the question, where is the inhibitory region binding site? It would appear from previous fluorescence and photo-cross-linking studies (Jha *et al.*, 1996; Kobayashi *et al.*, 1991, 1994, 1996; Lan *et al.*, 1989; Leavis *et al.*, 1984; Leszyk *et al.*, 1987, 1988, 1990; Leszyk *et al.*, 1998; Luo *et al.*, 1998, 1999, 2000a, 2000b; Ngai *et al.*, 1994; Tao *et al.*, 1989; Wang *et al.*, 1990), as well as the studies herein, that the two binding sites for $TnI_{1–40}$ and $TnI_{96–115}$ are very close in proximity such that the two sites may even be overlapping to some degree. Recent NMR spectroscopy studies analyzing the binding of $TnI_{96–115}$ and $TnI_{1–40}$ peptides with the C-domain of skeletal TnC observed the perturbance of some of the same residues of TnC when binding each peptide individually. For example, Mercier *et al.* (2000) observed residues Phe^{105}, Met^{158} and Gly^{160} to be similarly perturbed when binding each TnI peptide. However, a large number of charged residues Glu^{95}, Glu^{96}, Glu^{97}, Glu^{120}, Glu^{127} Glu^{132}, Arg^{123} and Lys^{139} are specifically perturbed by $TnI_{96–115}$ alone, indicating electrostatic binding of $TnI_{96–115}$ along the top and side of site III versus in the hydrophobic pocket of the C-domain as observed for $TnI_{1–40}$. Hence, the modulation of the inhibitory regions affinity for TnC by $TnI_{1–40}$ as discussed above may be by direct competition between some of the same residues and/or a very subtle conformational change of the same surrounding residues at site III.

The functional role of $TnI_{1–40}$'s negative effect on the binding of the regulatory region to TnC

Previous studies by Ngai and Hodges (1992) have demonstrated that a synthetic peptide corresponding to amino acids 1–40 of TnI can diminish TnC's ability to remove the inhibition of the actomyosin ATPase caused by either whole TnI or $TnI_{104–115}$ inhibitory peptide. More recently, Tripet *et al.* (1997) have also carried out competition studies and shown that the addition of $TnI_{1–40}$ resulted in the release of $TnI_{96–115}$ as well as of $TnI_{96–131}$, $TnI_{96–148}$ and TnI, albeit not as dramatically as observed by Ngai and Hodges (1992) to cause re-inhibition of the acto-Tm ATPase. In this study we also observed that the presence of $TnI_{1–40}$ could reduce the amount of $TnI_{96–139}$ (and $TnI_{96–131}$) in the ternary complex from 100% in its absence to ~70% in its presence [Fig. 6 (C)] and even greater at higher salt conditions. Thus the $TnI_{1–40}$ effect appears to be consistent.

Based on these observations, one can then ask the question what functional role the negative binding effect of $TnI_{1–40}$ on $TnI_{96–139}$ might play? The most obvious answer would be that the N-terminal region of TnI (1–40) may play a functional role in modulating the Ca^{2+}-sensitive release of TnI inhibition by TnC by weakening and facilitating the movements of TnI's inhibitory region between TnC and actin. Interestingly, Szczesna *et al.* (1996) have shown that a mutant TnC in which the Ca^{2+}/Mg^{2+} binding sites III/IV were 'knocked out' not only affected TnC retention in the troponin complex but also caused a leftward shift in the force-pCa relationship, i.e. activation could now occur at lower Ca^{2+} concentrations. Hence, the loss of $TnI_{1–40}$ interaction resulted in a greater affinity of the regulatory region for TnC (as observed in the absence of $TnI_{1–40}$ in the present study). Thus, the presence of the $TnI_{1–40}$ region indeed appears to be helping to zero in on the Ca^{2+} sensitivity range required for physiologically relevant regulation of the inhibitory region. There is also some speculation that the N-terminus of TnI may become phosphorylated under some conditions which may change its affinity for TnC, thus also affecting the regulatory regions affinity indirectly.

CONCLUSIONS

In summary, we have investigated the binding interactions between $TnI_{1–40}$ and TnC in the presence of Ca^{2+} ions, Mg^{2+} ions and the C-terminal regulatory region of TnI. We show that $TnI_{1–40}$ can bind with high affinity in the presence of both metal ions and in the presence of the regulatory region. The latter result illustrates that both regions of TnI (the N- and C-terminus) have separate binding sites on TnC. Thus, these results support the structural domain hypothesis which states that the N-terminus of TnI remains continuously bound to the C-domain of TnC at all times while the C-terminal regulatory region of TnI (~96–139) dynamically switches between the thin filament and its own sites on the N- and C-domain of TnC depending on the concentration of Ca^{2+}.

Acknowledgements

We thank Paul Semchuck and Morris Aarbo for technical assistance with peptide synthesis, purification, and isolation and of troponin C. We thank Kurt Wagschal, Colin Mant and Heman Chao for assistance with the

preparation of TnI-E-coil conjugates, and helpful discussions and comments on the preparation of the manuscript. We thank K. Oikawa for his skilled technical assistance in fluorescence spectroscopy. This research was supported by Sensium Technologies Inc., the University of Colorado Health Sciences Center, Denver, Colorado and an NIH grant to RSH (R01GM61855).

REFERENCES

Chong PC, Asselbergs PJ, Hodges RS. 1983. Inhibition of rabbit skeletal muscle acto-S1 ATPase by troponin T. *FEBS Lett.* **153**: 372–376.

Dalgarno D, Grand R, Levine B, Moir A, Scott G, Perry S. 1982. Interaction between troponin I and troponin C. *FEBS Lett.* **150**: 54–58.

De Crescenzo G, Grothe S, Lortie R, Debanne MT, O'Connor-McCourt M. 2000. Real-time kinetic studies on the interaction of transforming growth factor alpha with the epidermal growth factor receptor extracellular domain reveal a conformational change model. *Biochemistry* **39**: 9466–9476.

De Crescenzo G, Grothe S, Zwaagstra J, Tsang M, O'Connor-McCourt MD. 2001. Real-time monitoring of the interactions of transforming growth factor- beta (TGF-beta) isoforms with latency-associated protein and the ectodomains of the TGF-beta type II and III receptors reveals different kinetic models and stoichiometries of binding. *J. Biol. Chem.* **276**: 29632–29643.

Ding XL, Akella AB, Su H, Gulati J. 1994. The role of glycine (residue 89) in the central helix of EF-hand protein troponin-C exposed following amino-terminal alpha-helix deletion. *Protein Sci.* **3**: 2089–2096.

Drabikowski W, Dalgarno DC, Levine BA, Gergely J, Grabarek Z, Leavis PC. 1985. Solution conformation of the C-terminal domain of skeletal troponin C. Cation, trifluoperazine and troponin I binding effects. *Eur. J. Biochem.* **151**: 17–28.

Farah CS, Reinach FC. 1995. The troponin complex and regulation of muscle contraction. *Faseb J.* **9**: 755–767.

Farah CS, Miyamoto CA, Ramos CH, da Silva AC, Quaggio RB, Fujimori K, Smillie LB, Reinach FC. 1994. Structural and regulatory functions of the NH2- and COOH-terminal regions of skeletal muscle troponin I. *J. Biol. Chem.* **269**: 5230–5240.

Gagne SM, Tsuda S, Li MX, Smillie LB, Sykes BD. 1995. Structures of the troponin C regulatory domains in the apo and calcium- saturated states. *Nat. Struct. Biol.* **2**: 784–789.

Grabarek Z, Drabikowski W, Leavis PC, Rosenfeld SS, Gergely J. 1981. Proteolytic fragments of troponin C. Interactions with the other troponin subunits and biological activity. *J. Biol. Chem.* **256**: 13121–13127.

Herzberg O, James MN. 1985. Structure of the calcium regulatory muscle protein troponin-C at 2.8 A resolution. *Nature* **313**: 653–659.

Houdusse A, Love ML, Dominguez R, Grabarek Z, Cohen C. 1997. Structures of four Ca^{2+} bound troponin C at 2.0 A resolution: further insights into the Ca^{2+}-switch in the calmodulin superfamily. *Structure* **5**: 1695–1711.

Ingraham RH, Hodges RS. 1988. Effects of Ca^{2+} and subunit interactions on surface accessibility of cysteine residues in cardiac troponin. *Biochemistry* **27**: 5891–5898.

Jha PK, Mao C, Sarkar S. 1996. Photo-cross-linking of rabbit skeletal troponin I deletion mutants with troponin C and its thiol mutants: the inhibitory region enhances binding of troponin I fragments to troponin C. *Biochemistry* **35**: 11026–11035.

Johnsson B, Lofas S, Lindquist G. 1991. Immobilization of proteins to a carboxymethyldextran-modified gold surface for biospecific interaction analysis in surface plasmon resonance sensors. *Anal. Biochem.* **198**: 268–277.

Kobayashi T, Tao T, Grabarek Z, Gergely J, Collins JH. 1991. Cross-linking of residue 57 in the regulatory domain of a mutant rabbit skeletal muscle troponin C to the inhibitory region of troponin I. *J. Biol. Chem.* **266**: 13746–13751.

Kobayashi T, Tao T, Gergely J, Collins JH. 1994. Structure of the troponin complex. Implications of photocross-linking of troponin I to troponin C thiol mutants. *J. Biol. Chem.* **269**: 5725–5729.

Kobayashi T, Leavis PC, Collins JH. 1996. Interaction of a troponin I inhibitory peptide with both domains of troponin C. *Biochim. Biophys. Acta* **1294**: 25–30.

Kobayashi T, Zhao X, Wade R, Collins JH. 1999a. Ca^{2+}-dependent interaction of the inhibitory region of troponin I with acidic residues in the N-terminal domain of troponin C. *Biochim. Biophys. Acta.* **1430**: 214–221.

Kobayashi T, Zhao X, Wade R, Collins JH. 1999b. Involvement of conserved, acidic residues in the N-terminal domain of troponin C in calcium-dependent regulation. *Biochemistry* **38**: 5386–5391.

Kretsinger RH, Nockolds CE. 1973. Carp muscle calcium-binding protein. II. Structure determination and general description. *J. Biol. Chem.* **248**: 3313–3326.

Lan J, Albaugh S, Steiner RF. 1989. Interactions of troponin I and its inhibitory fragment (residues 104–115) with troponin C and calmodulin. *Biochemistry* **28**: 7380–7385.

Leavis PC, Gowell E, Tao T. 1984. Fluorescence lifetime and acrylamide quenching studies of the interactions between troponin subunits. *Biochemistry* **23**: 4156–4161.

Leszyk J, Collins JH, Leavis PC, Tao T. 1987. Cross-linking of rabbit skeletal muscle troponin with the photoactive reagent 4-maleimidobenzophenone: identification of residues in troponin I that are close to cysteine-98 of troponin C. *Biochemistry* **26**: 7042–7047.

Leszyk J, Collins JH, Leavis PC, Tao T. 1988. Cross-linking of rabbit skeletal muscle troponin subunits: labeling of cysteine-98 of troponin C with 4-maleimidobenzophenone and analysis of products formed in the binary complex with troponin T and the ternary complex with troponins I and T. *Biochemistry* **27**: 6983–6987.

Leszyk J, Grabarek Z, Gergely J, Collins JH. 1990. Characterization of zero-length cross-links between rabbit skeletal muscle troponin C and troponin I: evidence for direct interaction between the inhibitory region of troponin I and the NH2-terminal, regulatory domain of troponin C. *Biochemistry* **29**: 299–304.

Leszyk J, Tao T, Nuwaysir LM, Gergely J. 1998. Identification of the photocrosslinking sites in troponin-I with 4-maleimidobenzophenone labelled mutant troponin-Cs having single cysteines at positions 158 and 21. *J. Muscle Res. Cell Motil.* **19**: 479–490.

Li MX, Spyracopoulos L, Sykes BD. 1999. Binding of cardiac troponin-I147–163 induces a structural opening in human cardiac troponin-C. *Biochemistry* **38**: 8289–8298.

Luo Y, Wu JL, Gergely J, Tao T. 1998. Localization of Cys133 of rabbit skeletal troponin-I with respect to troponin-C by resonance energy transfer. *Biophys. J.* **74**: 3111–3119.

Luo Y, Leszyk J, Qian Y, Gergely J, Tao T. 1999. Residues 48 and 82 at the N-terminal hydrophobic pocket of rabbit skeletal muscle troponin-C photo-cross-link to Met121 of troponin-I. *Biochemistry* **38**: 6678–6688.

Luo Y, Leszyk J, Li B, Gergely J, Tao T. 2000a. Proximity relationships between residue 6 of troponin I and residues in troponin C: further evidence for extended conformation of troponin C in the troponin complex. *Biochemistry* **39**: 15306–15315.

Luo Y, Wu JL, Li B, Langsetmo K, Gergely J, Tao T. 2000b. Photocrosslinking of benzophenone-labeled single cysteine troponin I mutants to other thin filament proteins. *J. Mol. Biol.* **296**: 899–910.

McKay RT, Tripet BP, Hodges RS, Sykes BD. 1997. Interaction of the second binding region of troponin I with the regulatory domain of skeletal muscle troponin C as determined by NMR spectroscopy. *J. Biol. Chem.* **272**: 28494–28500.

McKay RT, Tripet BP, Pearlstone JR, Smillie LB, Sykes BD. 1999.

Defining the region of troponin-I that binds to troponin-C. *Biochemistry* **38**: 5478–5489.
Mercier P, Li MX, Sykes BD. 2000. Role of the structural domain of troponin C in muscle regulation: NMR studies of Ca^{2+} binding and subsequent interactions with regions 1-40 and 96-115 of troponin I. *Biochemistry* **39**: 2902–2911.
Ngai SM, Hodges RS. 1992. Biologically important interactions between synthetic peptides of the N- terminal region of troponin I and troponin C. *J. Biol. Chem.* **267**: 15715–15720.
Ngai SM, Hodges RS. 2001a. Characterization of the biologically important interaction between troponin C and the N-terminal region of troponin I. *J. Cell Biochem.* **83**: 99–110.
Ngai SM, Hodges RS. 2001b. Structural and functional studies on Troponin I and Troponin C interactions. *J. Cell Biochem.* **83**: 33–46.
Ngai SM, Sonnichsen FD, Hodges RS. 1994. Photochemical cross-linking between native rabbit skeletal troponin C and benzoylbenzoyl-troponin I inhibitory peptide, residues 104–115. *J. Biol. Chem.* **269**: 2165–2172.
Pearlstone JR, Sykes BD, Smillie LB. 1997. Interactions of structural C and regulatory N domains of troponin C with repeated sequence motifs in troponin I. *Biochemistry* **36**: 7601–7606.
Perry SV. 1999. Troponin I: inhibitor or facilitator. *Mol. Cell Biochem.* **190**: 9–32.
Potter JD, Gergely J. 1975. The calcium and magnesium binding sites on troponin and their role in the regulation of myofibrillar adenosine triphosphatase. *J. Biol. Chem.* **250**: 4628–4633.
Potter JD, Sheng Z, Pan BS, Zhao J. 1995. A direct regulatory role for troponin T and a dual role for troponin C in the Ca^{2+} regulation of muscle contraction. *J. Biol. Chem.* **270**: 2557–2562.
Ramakrishnan S, Hitchcock-DeGregori SE. 1995. Investigation of the structural requirements of the troponin C central helix for function. *Biochemistry* **34**: 16789–16796.
Sheng Z, Strauss WL, Francois JM, Potter JD. 1990. Evidence that both Ca(2+)-specific sites of skeletal muscle TnC are required for full activity. *J. Biol. Chem.* **265**: 21554–21560.
Sheng Z, Pan BS, Miller TE, Potter JD. 1992. Isolation, expression, and mutation of a rabbit skeletal muscle cDNA clone for troponin I. The role of the NH2 terminus of fast skeletal muscle troponin I in its biological activity. *J. Biol. Chem.* **267**: 25407–25413.
Slupsky CM, Sykes BD. 1995. NMR solution structure of calcium-saturated skeletal muscle troponin C. *Biochemistry* **34**: 15953–15964.
Slupsky CM, Shaw GS, Campbell AP, Sykes BD. 1992. A ^{1}H NMR study of a ternary peptide complex that mimics the interaction between troponin C and troponin I. *Protein Sci.* **1**: 1595–1603.
Sorenson MM, da Silva AC, Gouveia CS, Sousa VP, Oshima W, Ferro JA, Reinach FC. 1995. Concerted action of the high affinity calcium binding sites in skeletal muscle troponin C. *J. Biol. Chem.* **270**: 9770–9777.
Strynadka NC, Cherney M, Sielecki AR, Li MX, Smillie LB, James MN. 1997. Structural details of a calcium-induced molecular switch: X-ray crystallographic analysis of the calcium-saturated N-terminal domain of troponin C at 1.75 A resolution. *J. Mol. Biol.* **273**: 238–255.
Sundaralingam M, Bergstrom R, Strasburg G, Rao ST, Roy-Chowdhury P, Greaser M, Wang BC. 1985. Molecular structure of troponin C from chicken skeletal muscle at 3-angstrom resolution. *Science* **227**: 945–948.
Swenson CA, Fredricksen RS. 1992. Interaction of troponin C and troponin C fragments with troponin I and the troponin I inhibitory peptide. *Biochemistry* **31**: 3420–3429.
Syska H, Wilkinson JM, Grand RJ, Perry SV. 1976. The relationship between biological activity and primary structure of troponin I from white skeletal muscle of the rabbit. *Biochem. J.* **153**: 375–387.
Szczesna D, Guzman G, Miller T, Zhao J, Farokhi K, Ellemberger H, Potter JD. 1996. The role of the four Ca^{2+} binding sites of troponin C in the regulation of skeletal muscle contraction. *J. Biol. Chem.* **271**: 8381–8386.
Talbot JA, Hodges RS. 1981. Synthetic studies on the inhibitory region of rabbit skeletal troponin I. Relationship of amino acid sequence to biological activity. *J. Biol. Chem.* **256**: 2798–2802.
Tao T, Gowell E, Strasburg GM, Gergely J, Leavis PC. 1989. Ca^{2+} dependence of the distance between Cys-98 of troponin C and Cys- 133 of troponin I in the ternary troponin complex. Resonance energy transfer measurements. *Biochemistry* **28**: 5902–5908.
Tobacman LS. 1996. Thin filament-mediated regulation of cardiac contraction. *A. Rev. Physiol.* **58**: 447–481.
Tripet B, Van Eyk JE, Hodges RS. 1997. Mapping of a second actin-tropomyosin and a second troponin C binding site within the C terminus of troponin I, and their importance in the Ca^{2+}-dependent regulation of muscle contraction. *J. Mol. Biol.* **271**: 728–750.
Tripet B, DeCrescenzo G, Grothe S, O'Connor-McCourt M, Hodges RS. 2002. Kinetic analysis of the interactions between troponin C and the C-terminal troponin I regulatory region and validation of a new peptide delivery/capture system used for surface plasmon resonance. *J. Mol. Biol.* **323**: 345–362.
Tsuda S, Aimoto S, Hikichi K. 1992. 1H-NMR study of Ca(2+)-and Mg(2+)-dependent interaction between troponin C and troponin I inhibitory peptide (96–116). *J. Biochem. (Tokyo)* **112**: 665–670.
Van Eyk JE, Hodges RS. 1988. The biological importance of each amino acid residue of the troponin I inhibitory sequence 104–115 in the interaction with troponin C and tropomyosin-actin. *J. Biol. Chem.* **263**: 1726–1732.
Van Eyk JE, Strauss JD, Hodges RS, Ruegg JC. 1993. A synthetic peptide mimics troponin I function in the calcium-dependent regulation of muscle contraction. *FEBS Lett.* **323**: 223–228.
Van Eyk JE, Thomas LT, Tripet B, Wiesner RJ, Pearlstone JR, Farah CS, Reinach FC, Hodges RS. 1997. Distinct regions of troponin I regulate Ca^{2+}-dependent activation and Ca^{2+} sensitivity of the acto-S1-TM ATPase activity of the thin filament. *J. Biol. Chem.* **272**: 10529–10537.
Vassylyev DG, Takeda S, Wakatsuki S, Maeda K, Maeda Y. 1998. Crystal structure of troponin C in complex with troponin I fragment at 2.3-A resolution. *Proc. Natl Acad. Sci. USA* **95**: 4847–4852.
Wang ZY, Sarkar S, Gergely J, Tao T. 1990. Ca2(+)-dependent interactions between the C-helix of troponin-C and troponin-I. Photocross-linking and fluorescence studies using a recombinant troponin-C. *J. Biol. Chem.* **265**: 4953–4957.
Weeks RA, Perry SV. 1978. Characterization of a region of the primary sequence of troponin C involved in calcium ion-dependent interaction with troponin I. *Biochem. J.* **173**: 449–457.

